Journal of Medicinal Chemistry

Article

pubs.acs.org/jmc

Discovery and Characterization of GSK2801, a Selective Chemical Probe for the Bromodomains BAZ2A and BAZ2B

Peiling Chen,[§,○] Apirat Chaikuad,[†,○] Paul Bamborough,[∥] Marcus Bantscheff,[#] Chas Bountra,[‡] Chun-wa Chung,[∥] Oleg Fedorov,[†,‡] Paola Grandi,[#] David Jung,[§] Robert Lesniak,[§] Matthew Lindon,[⊥] Susanne Müller,[†,‡] Martin Philpott,[†,‡] Rab Prinjha,[⊥] Catherine Rogers,[†,‡] Carolyn Selenski,[§] Cynthia Tallant,[†,‡] Thilo Werner,[#] Timothy M. Willson,[§] Stefan Knapp,*[,†,‡,▽] and David H. Drewry*[,§]

[†]Nuffield Department of Clinical Medicine, Structural Genomics Consortium, University of Oxford, Old Road Campus Research Building, Roosevelt Drive, Headington, Oxford OX3 7DQ, United Kingdom

[‡]Nuffield Department of Clinical Medicine, Target Discovery Institute, University of Oxford, NDM Research Building, Roosevelt Drive, Headington, Oxford OX3 7FZ, United Kingdom

[§]Department of Chemical Biology, GlaxoSmithKline, Research Triangle Park, 5 Moore Drive, Research Triangle Park, North Carolina 27709-3398, United States

[∥]Computational & Structural Chemistry, Molecular Discovery Research, and [⊥]Epinova, Discovery Performance Unit, GlaxoSmithKline R&D, Stevenage, Hertfordshire SG1 2NY, United Kingdom

[#]Cellzome GmbH, Molecular Discovery Research, GlaxoSmithKline, Meyerhofstrasse 1, 69117 Heidelberg, Germany

[▽]Institute for Pharmaceutical Chemistry, Johann Wolfgang Goethe-University, Max-von-Laue-Str. 9, D-60438 Frankfurt am Main, Germany

Supporting Information

ABSTRACT: Bromodomains are acetyl-lysine specific protein interaction domains that have recently emerged as a new target class for the development of inhibitors that modulate gene transcription. The two closely related bromodomain containing proteins BAZ2A and BAZ2B constitute the central scaffolding protein of the nucleolar remodeling complex (NoRC) that regulates the expression of noncoding RNAs. However, BAZ2 bromodomains have low predicted druggability and so far no selective inhibitors have been published. Here we report the development of GSK2801, a potent, selective and cell active acetyl-lysine competitive inhibitor of BAZ2A and BAZ2B bromodomains as well as the inactive control compound GSK8573. GSK2801 binds to BAZ2 bromodomains with dissociation constants (K_D) of 136 and 257 nM for BAZ2B and BAZ2A, respectively. Crystal structures demonstrated a canonical acetyl-lysine competitive binding mode. Cellular activity was demonstrated using fluorescent recovery after photobleaching (FRAP) monitoring displacement of GFP-BAZ2A from acetylated chromatin. A pharmacokinetic study in mice showed that GSK2801 had reasonable *in vivo* exposure after oral dosing, with modest clearance and reasonable plasma stability. Thus, GSK2801 represents a versatile tool compound for cellular and *in vivo* studies to understand the role of BAZ2 bromodomains in chromatin biology.

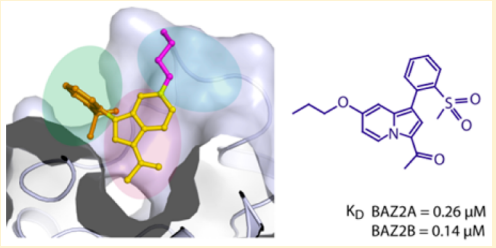

INTRODUCTION

Bromodomain modules selectively recognize acetylated lysine (KAc) containing sequences, a post-translational modification that is highly abundant in histones and other nuclear proteins.[1−3] Interest in these so-called epigenetic reader proteins has risen as it has become clear that the interaction between the proteins and the acetylated histone tails can be inhibited with small molecules. A number of reported selective bromodomain inhibitors are drug-like molecules and have potential as therapeutics in a range of diseases, including cancer and inflammation.[4−7] Much of the work to date has focused on the BET family for which inhibitors have now entered clinical testing.[4,8,9] The BET subfamily of bromodomains (BRDT and BRD2−4) has proven to be remarkably druggable. Interestingly, some molecules in clinical development[10−12] have been reported to have BET bromodomain binding activity in addition to their previously known activity. The rapid exploration of the biology of BET bromodomains has been facilitated by the availability of potent and selective small molecule chemical tools that have been widely used to study chromatin biology.[13−20] With that in mind, we embarked on efforts to identify probes for bromodomains outside of the BET subfamily through a public private partnership coordinated by the Structural Genomics Consortium. Here we outline the collaborative discovery of GSK2801, a chemical probe for the bromodomain adjacent to zinc finger domain protein (BAZ) 2A/B. An alternative

Special Issue: Epigenetics

Received: February 4, 2015
Published: March 23, 2015

DOI: 10.1021/acs.jmedchem.5b00209
J. Med. Chem. 2016, 59, 1410−1424

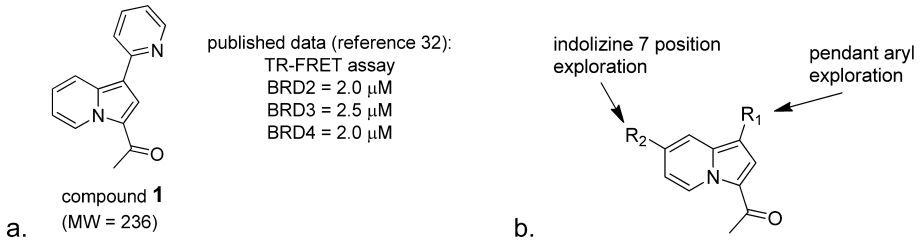

Figure 1. Initial hit and SAR strategy. (a) Structure of the initial hit compound **1**. (b) SAR development strategy targeting two positions (R1/R2) of the indolizine ring.

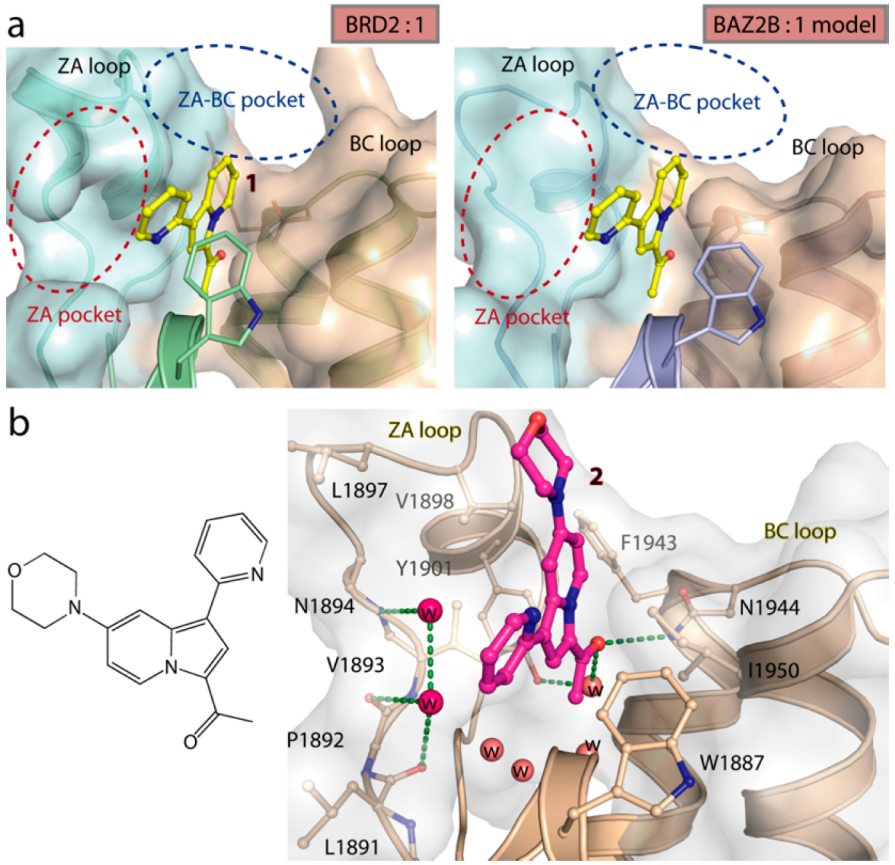

Figure 2. Cocrystal structure of compound **1** with BRD2 and compound **2** with BAZ2B. (a) Cocrystal structure of compound **1** with BRD2 and a model of compound **1** in BAZ2B. These illustrate that BRD2 appears to have a narrower channel that accommodates the pendant phenyl ring, suggesting this as an area to explore in order to enhance selectivity. (b) Chemical structure of compound **2** (left) and cocrystal structure of compound **2** with BAZ2B (right). The main interacting side chains are shown in ball and stick representation. Hydrogen bonds are shown as dotted lines. Conserved water molecules are depicted as spheres.

BAZ2A/B chemical probe that can be used as an additional independent validation tool has recently been published by our group in collaboration with an academic collaborator.[21]

BAZ1A, BAZ1B, BAZ2A, and BAZ2B constitute a family of evolutionarily conserved and ubiquitously expressed proteins with conserved domain structure including PHD and bromodomain histone tail reader motifs.[22] BAZ2A is a component of the nucleolar remodeling complex (NoRC), a member of the "imitation switch chromatin remodeling complexes" (ISWI),[23] which play a role in regulating the expression of noncoding RNAs and in the formation of repressive heterochromatin in particular at centromeres and telomeres.[24,25] Association of BAZ2A with acetylated histone tails is mediated by its bromodomain.[26] Recently, high expression levels of BAZA have been reported in prostate cancer, and the protein may serve as a marker for metastatic potential.[27]

Little is known about the BAZ2B subtype. However, single nucleotide polymorphisms (SNPs) in the *BAZ2B* gene locus have been associated with sudden cardiac death. High expression levels of BAZ2B have been associated with poor outcome of pediatric B cell acute lymphoblastic leukemia (B-ALL).[28] X-ray crystal structures of the BAZ2A/B bromodomains showed a shallow acetyl-lysine binding pocket, and they were predicted to be among the least druggable members of the protein family.[29] We therefore felt that identification of inhibitors for the BAZ2A/B bromodomains would be an interesting indicator of the chemical tractability of the broader protein family.

DOI: 10.1021/acs.jmedchem.5b00209
J. Med. Chem. 2016, 59, 1410−1424

Scheme 1. General Routes to Indolizines

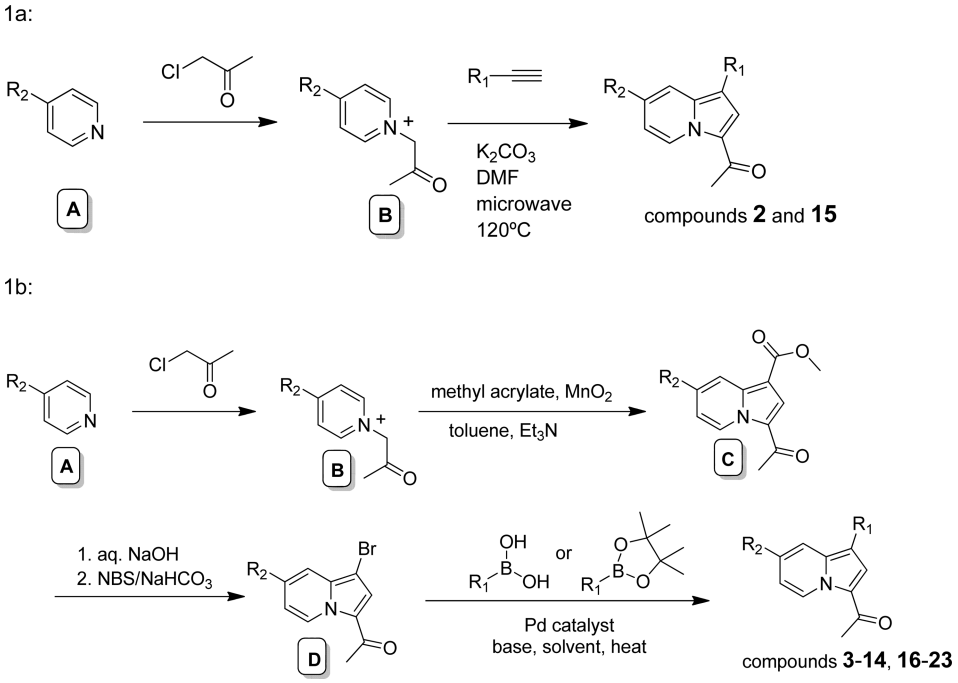

RESULTS AND DISCUSSION

A few weak binding acetyl-lysine mimetic fragments have been recently reported[30] in addition to a chemical tool compound, which showed an unusual aromatic π-stacking interaction of two aromatic moieties present in the inhibitor that efficiently filled out the binding pocket.[21] In our hands, screening of the BAZ2A bromodomain against a set of molecules that contained acetyl-lysine mimetics led to identification of a low molecular weight, chemically tractable indolizine, compound **1**, which had been previously reported as an inhibitor of BET bromodomain subfamily proteins. Indolizine **1** had a potency of 1.5 μM in a BAZ2A AlphaScreen assay, which was comparable to its reported activity against the BET bromodomains (Figure 1).[31,32]

A crystal structure of compound **1** bound to BRD2 (PDB ID: 4A9I) revealed that the methyl ketone is serving as an acetyl lysine mimetic (Figure 2A). Compound **1** was modeled into the acetyl lysine binding site of BAZ2B (Figure 2A). The channel that accommodates the indolizine R1 substituent appears wider in BAZ2B, suggesting that modification in this region will modulate selectivity. To facilitate the optimization of the indolizine hit, we cocrystallized an early representative compound (**2**) with BAZ2B (Figure 2B). Compound **2** has a 2-pyridyl group at R1 and a morpholine substituent in the R2 position. As is the case for compound **1** bound to BRD2,[2] the methyl ketone of compound **2** functions as an acetyl-lysine mimetic. The carbonyl forms a hydrogen bond with the conserved asparagine N1944 and with a network of water molecules that are typically found at the bottom of the acetyl-lysine binding site. The indolizine ring forms a number of hydrophobic interactions, most notably to I1950 and V1893. The aromatic ring in position R1 forms an aromatic stacking interaction with W1887. The R2 morpholino group was oriented toward the solvent and formed no significant interactions with BAZ2B. Details describing protein purification, crystallization, and crystallography as well as *in vitro* screening methods are available in the Supporting Information.

To optimize the indolizine hit for activity on BAZ2A/BAZ2B and selectivity over the BET bromodomains, we explored substituents at the 7-position of the indolizine and modified the aryl group at the 1-position. Compounds were synthesized via two general routes. In route 1 (Scheme 1a), an appropriately para-substituted pyridine **A** was *N*-alkylated with 1-chloropropan-2-one. The resulting pyridinium salt **B** was then reacted in a dipolar cycloaddition reaction with an aryl alkyne and potassium carbonate in DMF at elevated temperatures in a microwave to give the desired ring system with the acetyl lysine mimetic methyl ketone present in the 3-position of the indolizine. In route 2 (Scheme 1b), the appropriate pyridinium salt **B** was reacted with methyl acrylate in the presence of triethylamine and manganese dioxide in toluene at 90 °C for 1 h to give an indolizine **C** with a methyl ester in the 1-position, a methyl ketone in the 3-position, and the substituent that came from the starting pyridine in the 7-position. Saponification of the methyl ester with aqueous base, followed by bromination gave bromo-substituted indolizines of general structure **D**. In the final step, a Suzuki reaction was utilized to install the desired aryl group, R1, in the 1-position.

We first explored the structure–activity relationships (SARs) on the pendant phenyl group in the R1-position of the indolizine. In an AlphaScreen assay (Table 1), compounds **3**–**6** showed weaker activity at both BAZ2A and BAZ2B compared to **1**. Replacing the pendant 2-pyridyl group with a *meta*-methoxy phenyl (compound **3**) obliterated activity at both BAZ2A and BAZ2B. Compound **7**, harboring an *ortho*-CH_2OH, maintained activity at BAZ2A and gave a good increase in potency at BAZ2B, moving from 7 to 1 μM. Compound **12**, which incorporates an *ortho*-methyl sulfone, improved potency on BAZ2A to 720 nM, and BAZ2B stayed in the low micromolar IC_{50} range.

Based on the improved potency of the compounds on both BAZ2A and BAZ2B with the *ortho*-CH_2OH compound **7** and the *ortho*-methyl sulfone **12**, we explored substitution on the indolizine ring with these groups in place. In the context of the *ortho*-CH_2OH substituted pendant phenyl (Table 2), a methyl

DOI: 10.1021/acs.jmedchem.5b00209
J. Med. Chem. 2016, 59, 1410–1424

Table 1. Substitution on the Pendant Phenyl Ring; Shown Are Averaged Values of Three Replicates and the Standard Error of the Mean (SEM)

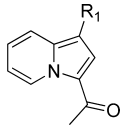

compd	R1	BAZ2A IC_{50} (μM)	BAZ2B IC_{50} (μM)
1	2-pyridyl	1.5 ± 0.06	7.0 ± 0.03
3	*m*-methoxy-phenyl	>30	>30
4	2-thiophene	8.6 ± 0.01	34.1 ± 0.19
5	*o*-OH-phenyl	7.2 ± 0.06	22.7 ± 0.5
6	*m*-OH-phenyl	3.3 ± 0.05	12.5 ± 0.04
7	*o*-CH_2OH-phenyl	1.8 ± 0.05	1.0 ± 0.02
8	*m*-$CONH_2$-phenyl	1.8 ± 0.02	9.8 ± 0.06
9	*o*-CH_2OH, *p*-OMe-phenyl	1.4 ± 0.01	1.5 ± 0.03
10	*p*-CH_2OH-phenyl	1.2 ± 0.07	4.1 ± 0.02
11	*p*-NMe_2-phenyl	1.1 ± 0.07	3.8 ± 0.03
12	*o*-methyl sulfone-phenyl	0.72 ± 0.07	1.3 ± 0.04

Table 2. Influence of the 7-Position Indolizine Substitution in the Context of the *ortho*-CH_2OH on the Pendant Phenyl Ring; Shown Are Averaged Values of Three Replicates and the Standard Error of the Mean (SEM)

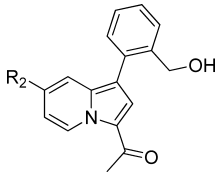

compd	R2	BAZ2A IC_{50} (μM)	BAZ2B IC_{50} (μM)
7	H	1.8 ± 0.05	1.0 ± 0.02
13	CH_3	1.0 ± 0.09	0.37 ± 0.02
14	OCH_3	1.2 ± 0.01	0.41 ± 0.03
15	morpholine	1.7 ± 0.13	0.54 ± 0.05
16	$CONH_2$	4.1 ± 0.09	1.90 ± 0.01
17	OPh	4.1 ± 0.06	0.61 ± 0.01

group **13** and a methoxy group **14** improved BAZ2A activity relative to the unsubstituted parent, compound **7**. Both the primary carboxamide substituted indolizine **16** and the phenoxy substituted compound **17** were weaker against BAZ2A. BAZ2B activity was improved in methyl substituted indolizine **13**, methyl ether substituted indolizine **14**, morpholine substituted indolizine **15**, and phenyl ether substituted indolizine **17**. With amide substituted compound **16**, however, we saw a potency decrease on BAZ2A relative to unsubstituted compound **7**.

Within a series of *ortho*-methyl sulfone phenyl analogues (Table 3), several indolizine substituents improved activity at both BAZ2A and BAZ2B relative to unsubstituted compound **12**. The Boc-protected aminomethyl substituent **18** gave good potency increases. In the *ortho*-hydroxymethyl series described in Table 2, ethers off of the indolizine helped BAZ2B activity but in general were less helpful for BAZ2A activity. In the *ortho*-methylsulfone context, however, the methyl ether **21**, propyl ether **19**, and phenyl ethers **20** enhanced both BAZ2A and BAZ2B activity.

Following identification of a handful of compounds with improved potencies, we sought to characterize their activity at other bromodomains. Table 4 shows that the two unsubstituted

Table 3. Seven-Position Indolizine Substitution in the Context of the *ortho*-SO_2Me on the Pendant Phenyl Ring; Shown Are Averaged Values of Three Replicates and the Standard Error of the Mean (SEM)

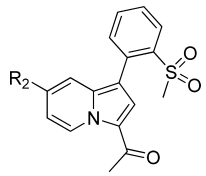

compd	R2	BAZ2A IC_{50} (μM)	BAZ2B IC_{50} (μM)
12	H	0.72 ± 0.07	1.3 ± 0.04
18	CH_2NH-Boc	0.16 ± 0.05	0.67 ± 0.02
19	OPr	0.40 ± 0.03	0.43 ± 0.02
20	OPh	0.55 ± 0.00	0.84 ± 0.04
21	OMe	0.58 ± 0.05	0.82 ± 0.01
22	Me	0.89 ± 0.00	1.9 ± 0.04

indolizines **7** and **12** were quite weak on BRD4 and BRD9. The Boc-protected aminomethyl compound **18**, however, has low micromolar BRD9 activity and thus is not suitable as a BAZ2B/A probe. The ethers (**19**–**21**) were inactive or very weakly active against BRD4(1) and BRD9.

Modeling suggested that the improved selectivity of the bulkier ortho-substituted phenyls for BAZ2B over BET resulted from reduced planarity of these compounds with respect to *ortho*-H and 2-pyridyl analogues. The binding site of BRD2 is narrower than BAZ2B and binds compound **1** in essentially a planar conformation (Figure 2A). Docking of compounds **17** and **20** into the BRD2 site gave strained, high-energy poses consistent with their lower *in vitro* potency. In contrast, the more open site of BAZ2B was able to accommodate docked o-substituted phenyl indolizines with ease.

We cocrystallized compounds **17** and **20** with BAZ2B (Figure 3). The structure confirmed that the introduction of the 2-hydroxyl-methyl group at the phenyl ring produced a 90° rotation of the phenyl ring incompatible with potent BET binding. In BAZ2B, the rotated phenyl ring makes an end-on π-stacking interaction with W1887 and orients the 2-hydoxyl-methyl group to produce a hydrogen-bond with the ZA-loop backbone (N1894 amine). The methyl-sulfonyl substitution at position-2 of the phenyl ring produces an even more dramatic rotation to accommodate the more bulky sulfonyl group. In addition, the sulfonyl oxygen groups also make a pair of hydrogen bonds to the backbone NH of N1894.

Based on the potency and excellent selectivity over the BET bromodomains, we chose to look at compound **19**, GSK2801, in more detail. We wanted to determine the potency of the compound in orthogonal assay systems. The interaction between the small molecule GSK2801 and the bromodomain was examined using biolayer interferometry (Octet-RED BLI) and isothermal titration calorimetry (ITC) (Figure 4a,b). Steady state fits of the measured dose response BLI data resulted in a dissociation constant of 60 nM (K_D). The inhibitor showed fast on- and off-rate binding (K_{on}, 1.57 ± 0.02 × 10^5 1/(M s); K_{off}, 6.95 ± 0.058 × 10^{-3} 1/s). ITC confirmed this value determining a K_D of 136 and 257 nM for BAZ2B and BAZ2A and a stoichiometry of 1.0 ± 0.1, respectively. The cocrystal structure with GSK2801 showed that the observed binding mode of the probe is conserved when compared with the related compound **20** (Figure 4c).

DOI: 10.1021/acs.jmedchem.5b00209
J. Med. Chem. 2016, 59, 1410−1424

Table 4. Cross Screening of Most Potent BAZ Compounds on BRD4(1) and BRD9; Shown Are Averaged Values of Three Replicates and the Standard Error of the Mean (SEM)

compd	indolizine substituent	pendant phenyl substituent	BAZ2A IC_{50} (μM)	BAZ2B IC_{50} (μM)	BRD4 IC_{50} (μM)	BRD9 IC_{50} (μM)
7	H	*o*-CH_2OH	1.8 ± 0.05	1.0 ± 0.02	38.9 ± 13.3	23.7 ± 0.16
12	H	*o*-SO_2Me	0.72 ± 0.07	1.3 ± 0.04	>50	17.9 ± 3.85
18	CH_2NH-Boc	*o*-SO_2Me	0.16 ± 0.11	0.67 ± 0.03	>50	1.4 ± 0.04
19	OPr	*o*-SO_2Me	0.40 ± 0.03	0.43 ± 0.02	>50	>50
20	OPh	*o*-SO_2Me	0.55 ± 0.0	0.84 ± 0.04	>50	19.9 ± 1.84
21	OMe	*o*-SO_2Me	0.58 ± 0.05	0.82 ± 0.01	>50	>50

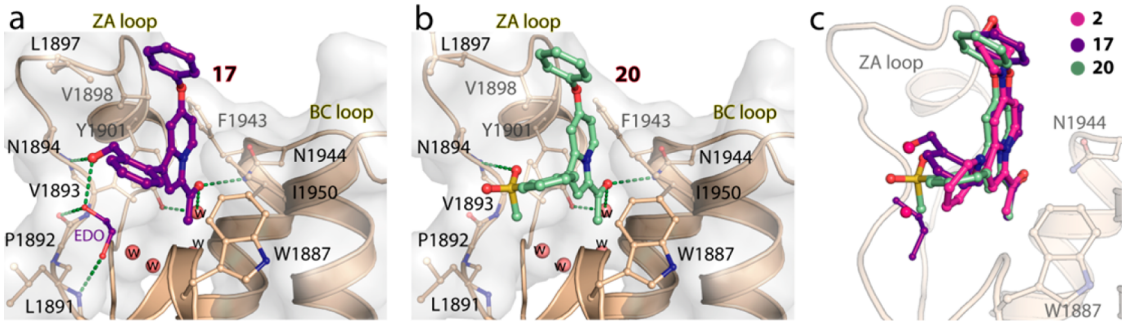

Figure 3. Cocrystal structure of compounds **17** and **20** with BAZ2B. (a) Cocrystal structure with compound **17**. (b) Cocrystal structure with compound **20**. Orientation and labeling are identical to those in Figure 2. (c) Superimposition of cocrystal structures with compounds **2**, **17**, and **20**. Compounds were well-defined by electron density. Ligand omitted electron density maps have been included in the Supporting Information.

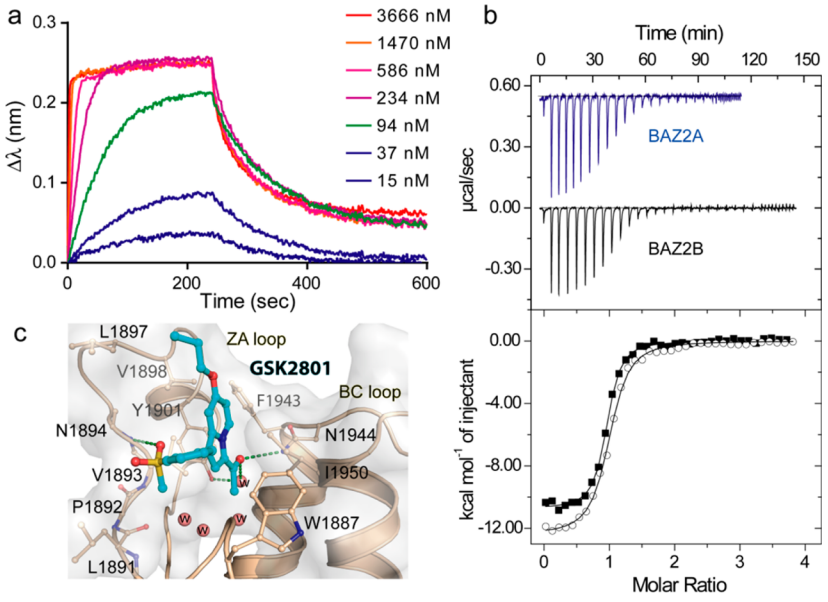

Figure 4. Affinity and binding mode of the BAZ2A/B chemical probe GSK2801. (a) Dose response biolayer interference (BLI) data measuring the binding kinetics of GSK2801 to BAZ2B. Steady state fitting resulted in a K_d value of 60 nM. (b) Isothermal titration calorimetry (ITC) binding experiments for the interaction of GSK2801 with BAZ2A (blue in top panel and circles in lower panel) and BAZ2B (black in top panel and squares in lower panel), respectively. Raw data heats are shown in the top panel. The lower panel shows normalized binding heats and the fitted function to a single binding site model. (c) Cocrystal structure with BAZ2B. The structure is depicted in similar orientation to that in Figure 3.

Next we assessed the wider selectivity of GSK2801 against other bromodomains in thermal stability assays. BAZ2A/B bromodomains are exceptionally stable interaction domains, a property that resulted in small temperature shifts in thermal stability assays even in the presence of tightly binding ligands. At an inhibitor concentration of 10 μM, GSK2801 resulted in a temperature shift of 4.1 and 2.7 °C for BAZ2A and BAZ2B, respectively. Significant T_m shifts were also observed for the second bromodomain in TAF1L(2) (3.4 °C) and BRD9 (2.3 °C) (Figure 5a).

Because of the limited sensitivity of BAZ2A/B in the thermal stability assay we evaluated the selectivity of GSK2801 using an alternative assay format. Forty-two bromodomains modified with a Bir A biotin ligase targeting sequence were coexpressed in bacteria with the enzyme. This coexpression strategy resulted in homogeneously biotin-labeled bromodomains *in vivo*.[33] The successful labeling with biotin was verified using mass spectrometry (data not shown). We used the biotinylated proteins in BLI experiments probing the interaction of GSK2801 at two concentrations (0.2 and 1.0 μM) (Figure 5b). In agreement

DOI: 10.1021/acs.jmedchem.5b00209
J. Med. Chem. 2016, 59, 1410−1424

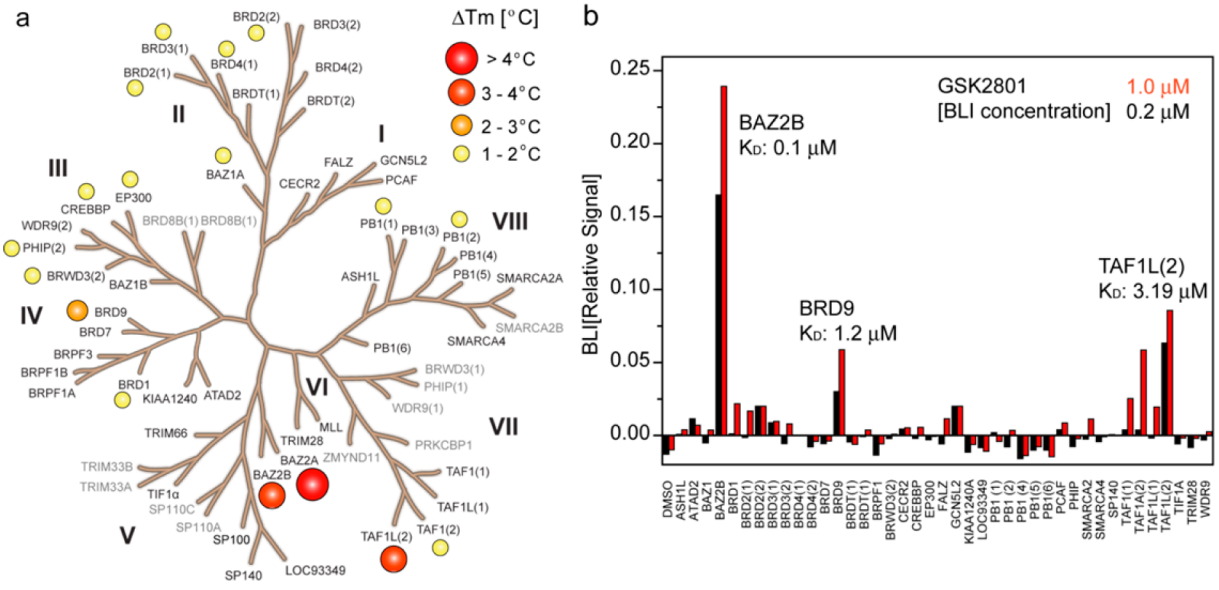

Figure 5. GSK2801 selectivity against the bromodomain family. (a) Temperature shift data (ΔT_m) cross screening against a panel of 46 human bromodomains. Screened targets are shown in bold. Temperature shifts are shown as indicated in the figure. (b) Selectivity screening using biolayer interferometry and a panel of 40 biotin-labeled proteins. Screening was carried out at two inhibitor concentrations (1.0 and 0.2 μM) as indicated in the figure. ITC K_D data for the most significant hits are also shown.

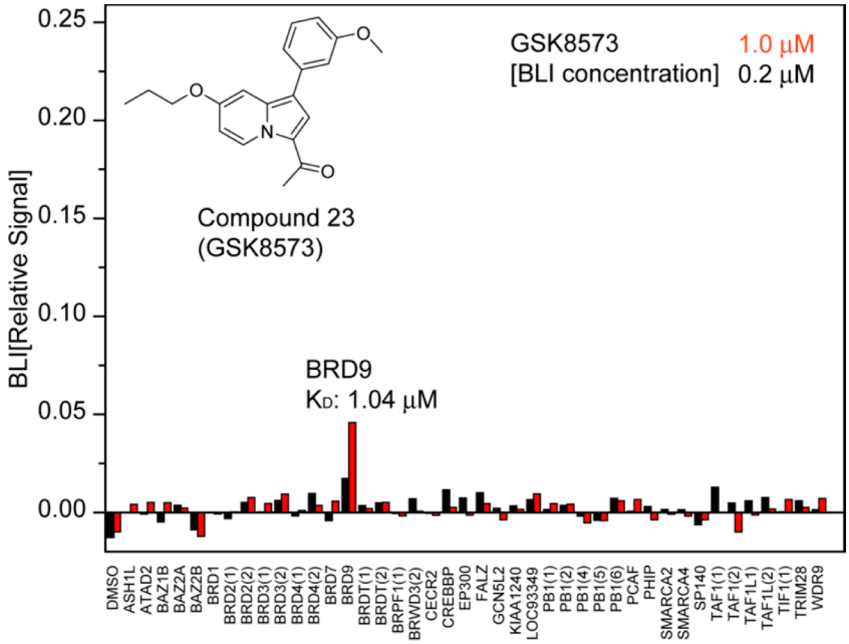

Figure 6. Structure of the inactive control compound GSK8573 and family wide screening of biotin labeled bromodomains using BLI. BLI experiments were performed at two concentrations (1.0 and 0.2 μM). The scale of the *y*-axis is identical to the one used in Figure 5b.

with the ΔT_m data, BRD9 and TAF1(L) were detected as the major off-targets, while no other significant interactions were detected within the bromodomain family.

We quantified the off-target interactions using ITC. These experiments showed that GSK2801 bound TAF1L(2) with an affinity K_B of 0.31 ($\pm$ 0.02) $\times$ 10^6 M^{-1} (K_D: 3.2 μM) and a binding enthalpy change ΔH of -8.6 ($\pm$0.02) kcal/mol. ITC experiments using the bromodomain of BRD9 resulted in the determination of an affinity K_B of 0.826 ($\pm$0.02) $\times$ 10^6 M^{-1} (K_D: 1.1 μM) and ΔH of -9.8 ($\pm$0.01) kcal/mol. TAF1L is a retrotransposed gene only present in the primate lineage that has a very restricted expression to the testis compartment.[34] However, TAF1L has been reported to be mutated and expressed in a subset of melanoma cases.[35] BRD9 is expressed in most tissues and is an off-target of GSK2801.

Because of the off-target activity with BRD9, we developed a structurally highly related control compound that lacked activity on BAZ2A/B. Based on the low activity on BAZ2A and BAZ2B with a *meta*-methoxy substituted pendant phenyl (compound **3**), we designed a compound that utilized this moiety in conjunction with the propyl ether in the indolizine 7-position. Using the established BLI cross-screening assay format, this compound (compound **23**, GSK8573) proved to be inactive against BAZ2A/B and all other bromodomains except BRD9 (Figure 6).

DOI: 10.1021/acs.jmedchem.5b00209
J. Med. Chem. 2016, 59, 1410−1424

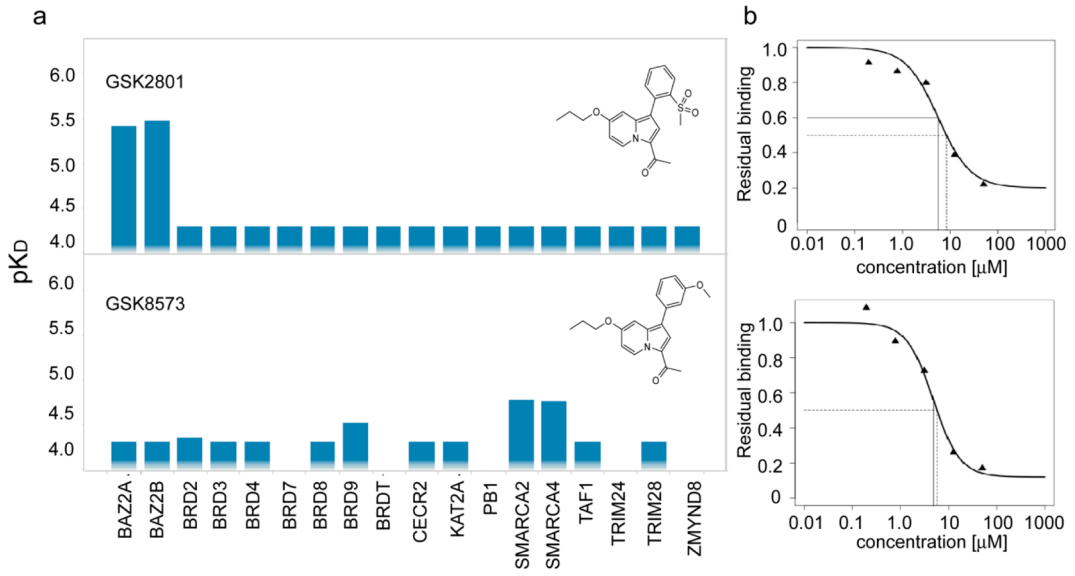

Figure 7. Chemoproteomic profiling of BAZ inhibitor selectivity to endogenous bromodomain proteins. (a) pK_ds of GSK2801 and GSK8573 (negative control) for BAZ2A, BAZ2B, and 16 additional BRD proteins captured on the GSK2801 affinity matrix from HuT-78 cell lysate. (b) Dose response curves of GSK2801 for BAZ2A (top) and BAZ2B (bottom) in the same assay.

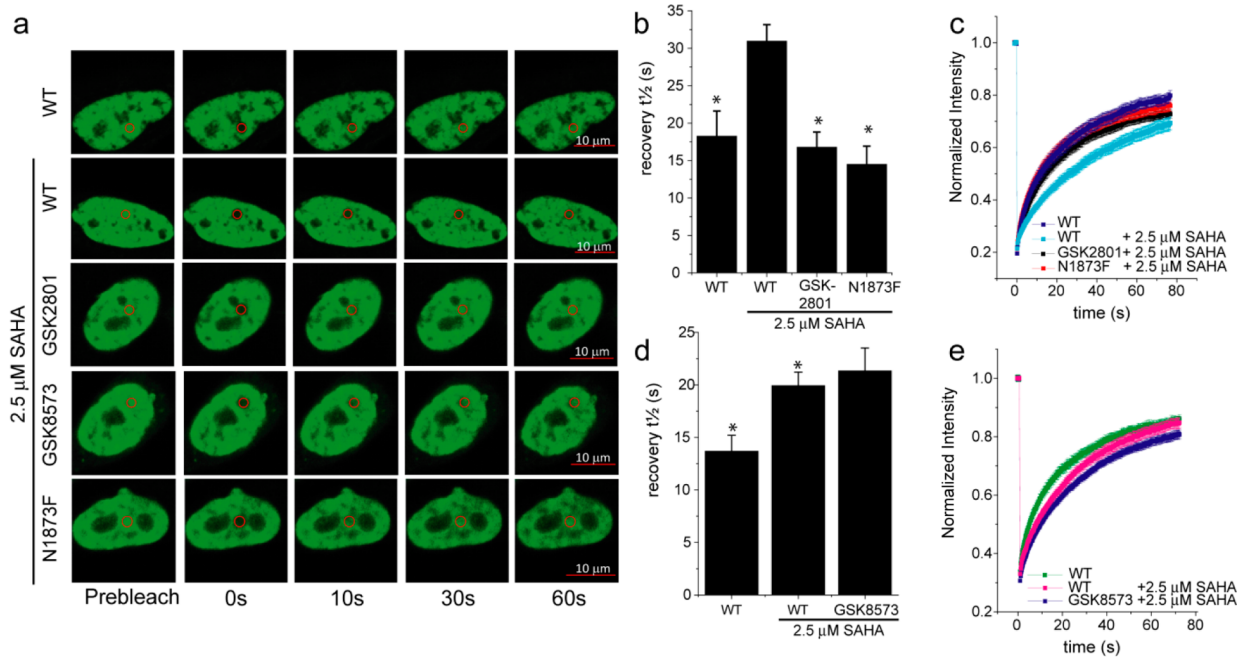

Figure 8. BAZ2A fluorescence recovery after photobleaching assay. (a) Images of nuclei of BAZ2A-GFP transfected cells. The bleached area is indicated by a red circle. Shown is the time dependence of the fluorescent recovery of WT BAZ2A and the bromodomain inactivating mutant N1873F in the presence and absence of GSK2801 and the BAZ2A/BAZ2B inactive control compound GSK8573. (b) Half times of fluorescence recovery ($t_{1/2}$) for BAZ2A are shown as bars representing the mean $t_{1/2}$ calculated from individual recovery curves of at least 10 cells per group, and error bars depict the standard error of the mean (SEM). (c) Raw data fluorescent recovery curves corresponding to the fluorescence recovery shown in panel a. (d) FRAP measured on the control compound GSK8573. (e) Corresponding fluorescent recovery curves. *$p < 0.05$ compared to WT treated with 2.5 μM SAHA.

Using ITC we determined an affinity for interaction of GSK8573 with BRD9 of 1.04 μM (K_D) associated with a favorable binding enthalpy change ΔH of −8.98 (± 0.152) kcal/mol. Thus, GSK8573 shared similar affinity for the off-target BRD9 while losing all activity against the rest of the bromodomain family. These results suggest that GSK8573 can be used as a structurally related negative control compound in biological experiments.

To test whether GSK2801 would also bind to endogenous BAZ2 proteins, we devised a chemoproteomic competition binding assay. The Boc-protecting group of compound **18** was removed to provide an amine functionalized analogue of GSK2801 that was immobilized on sepharose beads. The resulting affinity matrix was incubated with nuclear and chromatin enriched HuT78 extracts containing increasing concentrations of GSK2801 or the structurally related GSK8573. Bound proteins were eluted and quantified using an isobaric mass tagging strategy and targeted mass spectrometry.[36,37] Among the 18 endogenous full-length bromodomain proteins that bound to

DOI: 10.1021/acs.jmedchem.5b00209
J. Med. Chem. 2016, 59, 1410−1424

the matrix, only BAZ2A and BAZ2B displayed a dose-dependent reduction binding by GSK2801 suggesting a low micromolar potency ($pK_d = 5.5$) (Figure 7a,b). Conversely, GSK8573 did not show any binding to BAZ2 proteins up to a concentration of 50 μM, but limited affinity to BRD9 ($pK_d = 4.5$) and to SMARCA2 and 4 ($pK_d = 4.8$), which is likely to be indirect due to the association of SMARCA2 and 4 to BRD9 in the BAF complex[38] (Figure7a).

In order to determine if GSK2801 could displace the BAZ2A/B from chromatin in cells we utilized FRAP experiments. Treatment of U2OS cells with the HDAC inhibitor SAHA induced hyperacetylated chromatin and a better activity window in the FRAP assay. SAHA-treated U2OS cells were transfected with a GFP-BAZ2A fusion construct. In parallel, U2OS cells were transfected with a GFP fusion with a BAZ2A mutant construct (N1873F) in which the conserved asparagine essential for recognizing the acetylated lysine had been mutated (Figure 8). GSK2801 accelerated FRAP half-recovery time to the same extent as observed for the mutant construct indicating that the compound was able to displace BAZ2A from chromatin. Conversely, the inactive GSK-8573 did not have any effect on the half-recovery time of GFP-BAZ2A.

In order to determine the suitability of GSK2801 for *in vivo* experiments we measured pharmacokinetic parameters after intraperitoneal and oral dosing to male CD1 mice. This pharmacokinetics study showed that GSK2801 has reasonable *in vivo* exposure after oral dosing, modest clearance, and reasonable plasma stability (Figure 9). These properties should allow GSK2801 to be used as a BAZ2A/B bromodomain inhibitor *in vivo*.

CONCLUSION

In this article, we started from an unselective micromolar BAZ/BET inhibitor and optimized it through iterative medicinal chemistry to a potent inhibitor of BAZ2A/B with >50-fold selectivity over BRD4. X-ray crystallography has provided a convincing rationalization of the steric features resulting in the BET selectivity. The resulting molecule, GSK2801, is a potent and selective ligand for the BAZ2A and BAZ2B bromodomains, suitable for use as a small molecule chemical probe. GSK2801 has excellent selectivity for BAZ2A and BAZ2B, with only low micromolar residual activity at BRD9 and TAF1L. The compound displaces full length GFP-BAZ2A from chromatin at concentrations below 1 μM. We have also identified a closely related inactive control compound to help inform cellular screening results. In order to accelerate discoveries on the roles of BAZ2B and BAZ2A in physiology and pathophysiology, we are sharing these compounds with the research community.

EXPERIMENTAL SECTION

Chemistry. All solvents and commercial chemicals were reagent grade and used without purification. The purity of final compounds was determined by HPLC/MS and ^{1}H NMR and determined to be >95%. ^{1}H NMR spectra were recorded on Bruker BioSpin spectrometer operating at 400 mHz in $CDCl_3$, methanol-d_4, or DMSO-d_6. The chemical shifts (δ) reported are given in parts per million (ppm), and the coupling constants (J) are in hertz (Hz). The spin multiplicities are reported as s = singlet, br s = broad singlet, d = doublet, t = triplet, q = quartet, m = multiplet, and br = broad.

The LC/MS analysis was performed on a Waters SQD with a Phenomenex Kinetex 1.7 μm XB-C18 column at 40 °C, using water + 0.2% v/v formic acid and acetonitrile + 0.15% v/v formic acid as mobile phase, and performed on Waters Acquity BEH C18 2 × 50 mm 1.7 m column at 50 °C, using water + 0.20% v/v formic acid, water + 0.20% v/v formic acid, and acetonitrile + 0.15% v/v formic acid. Microwave irradiated reactions were carried out in sealed glass vessels in a Biotage Initiator. Flash chromatography purifications were carried out on a Biotage SP1 instrument.

Synthesis of Compound 19 (GSK2801): 1-(1-(3-(Methylsulfonyl)-phenyl)-7-propoxyindolizin-3-yl)ethanone. Route 1:

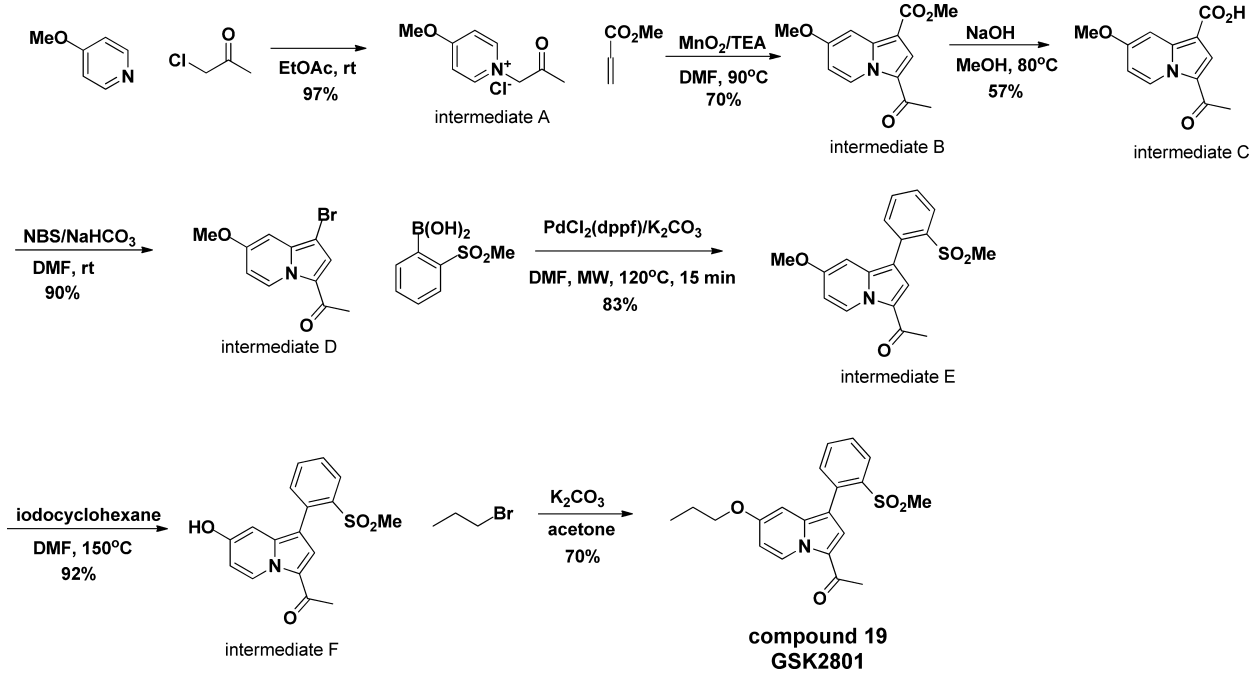

*Synthesis of Compound **19** (GSK2801) Intermediate A.* A mixture of 4-methoxypyridine (5 g, 45.8 mmol) and 1-chloropropan-2-one (18.43 mL, 229 mmol) in ethyl acetate (50 mL) was stirred at 80 °C for 2 h. The mixture was concentrated to dryness to give 4-methoxy-1-(2-oxopropyl)pyridin-1-ium chloride (9 g, 44.6 mmol, 97% yield) as a yellow solid.

*Synthesis of Compound **19** (GSK2801) Intermediate B.* To a suspension of 4-methoxy-1-(2-oxopropyl)pyridin-1-ium chloride (5.14 g,

DOI: 10.1021/acs.jmedchem.5b00209
J. Med. Chem. 2016, 59, 1410−1424

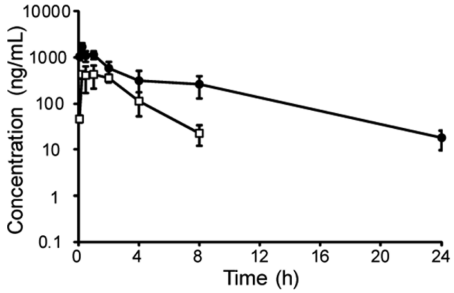

PK parameter for GSK2801 in mice	
IP (30mg/kg)	PO (30mg/kg)
T_{max}: 0.25 h	T_{max}: 1.0 h
C_{max}: 1670 ng/mL	C_{max}: 435 ng/mL
Terminal $t_{1/2}$: 4.5 h	Terminal $t_{1/2}$: 1.5 h

Figure 9. Pharmacokinetic properties of GSK2801 in mice. The figure shows the mean plasma concentration of GSK2801 in mice ($n = 3$) after oral (PO) (circles) and intraperitoneal (IP) (squares) dosing (30 mg/kg).

25.5 mmol) in toluene (60 mL) was added methyl acrylate (22.93 mL, 255 mmol), TEA (5.33 mL, 38.2 mmol), and then manganese dioxide (17.73 g, 204 mmol). The mixture was stirred at 90 °C for 1 h. The solid was filtered off over Celite and washed with acetone. The combined filtrate was concentrated and purified by silica gel chromatography eluting with EtOAc in hexanes (5 to 50%) to give methyl 3-acetyl-7-methoxyindolizine-1-carboxylate (4.4 g, 17.80 mmol, 69.8% yield) as a yellow solid.

Synthesis of Compound ***19*** *(GSK2801) Intermediate C.* To a solution of methyl 3-acetyl-7-methoxyindolizine-1-carboxylate (4.4 g, 17.80 mmol) in methanol (60 mL) was added NaOH (44.5 mL, 178 mmol). The mixture was stirred at 80 °C for 30 min. The solution was concentrated and acidified with 6 N HCl to pH = 1. The solid product was filtered, washed with water, and dried to give 3-acetyl-7-methoxyindolizine-1-carboxylic acid (2.4 g, 10.29 mmol, 57.8% yield) as a yellow solid. The product was used in the next step without further purification.

Synthesis of Compound ***19*** *(GSK2801) Intermediate D.* To a slurry of 3-acetyl-7-methoxyindolizine-1-carboxylic acid (2.4 g, 10.29 mmol) in *N*,*N*-dimethylformamide (DMF) (100 mL) was added sodium bicarbonate (2.59 g, 30.9 mmol) and then NBS (1.923 g, 10.81 mmol) portionwise at 0 °C. The mixture was stirred at ambient temperature for 1.5 h. The solution was treated with water and extracted with EtOAc. The combined organics were washed with water, brine, dried over Na_2SO_4, and filtered. The filtrate was concentrated to dryness to give 1-(1-bromo-7-methoxyindolizin-3-yl)ethanone (2.5 g, 9.32 mmol, 91% yield). The product was used in the next step without further purification.

Synthesis of Compound ***19*** *(GSK2801) Intermediate E.* Nitrogen gas was bubbled through a mixture of 1-(1-bromo-7-methoxyindolizin-3-yl)ethanone (515 mg, 1.921 mmol), $PdCl_2(dppf)-CH_2Cl_2$ adduct (110 mg, 0.134 mmol), K_2CO_3 (796 mg, 5.76 mmol), and (2-(methylsulfonyl)phenyl)boronic acid (768 mg, 3.84 mmol) in DMF (4 mL) and water (0.5 mL) for 10 min. Then the mixture was heated in a sealed tube in the microwave (120 °C, 25 min). The solution was extracted with EtOAc, and the combined organics were washed with water, brine, dried over Na_2SO_4, and filtered. The filtrate was concentrated, then purified using silica gel chromatography, eluting with EtOAc in hexanes (20 to 60%) to give 1-(7-methoxy-1-(2-(methylsulfonyl)phenyl)indolizin-3-yl)ethanone (368 mg, 1.072 mmol, 55.8% yield) as a light yellow solid.

Synthesis of Compound ***19*** *(GSK2801) Intermediate F.* To a solution of 1-(7-methoxy-1-(2-(methylsulfonyl)phenyl)indolizin-3-yl)-ethanone (368 mg, 1.072 mmol) in DMF (5 mL) was added iodocyclohexane (0.693 mL, 5.36 mmol). The mixture was stirred at 155 °C for 12 h. The mixture was treated with sodium thiosulfate ($Na_2S_2O_3$) and extracted with EtOAc. The combined organics were washed with water, brine, dried over Na_2SO4, and filtered. The filtrate was concentrated to dryness to give 1-(7-hydroxy-1-(2-(methylsulfonyl)-phenyl)indolizin-3-yl)ethanone (325 mg, 0.987 mmol, 92% yield). The crude product was used in the next step without further purification.

Compound 19 (GSK2801): 1-(1-(3-(Methylsulfonyl)phenyl)-7-propoxyindolizin-3-yl)ethanon. A mixture of 1-(7-hydroxy-1-(3-(methylsulfonyl)phenyl)indolizin-3-yl)ethanone (38 mg, 0.115 mmol), K_2CO_3 (19.13 mg, 0.138 mmol), and 1-bromopropane (0.210 mL, 2.307 mmol) in acetone (1.5 mL) was stirred at 75 °C for 2 h. The product was purified by reverse phase HPLC (35 to 100% acetonitrile in water for 6 min and 100% acetonitrile for 1 min, with 0.05% TFA as additive) to give 1-(1-(3-(methylsulfonyl)phenyl)-7-propoxyindolizin-3-yl)ethanone (30 mg, 0.081 mmol, 70.0% yield) as a colorless solid.

^{1}H NMR (400 MHz, chloroform-*d*) δ ppm 1.04 (t, $J = 7.28$ Hz, 3 H), 1.70−1.92 (m, 2 H), 2.57 (s, 3 H), 2.68 (s, 3 H), 3.89 (t, $J = 6.27$ Hz, 2 H), 6.60 (s, 1 H), 6.68 (d, $J = 7.53$ Hz, 1 H), 7.51 (d, $J = 7.28$ Hz, 1 H), 7.56−7.64 (m, 1 H), 7.67−7.74 (m, 1 H), 7.81 (s, 1 H), 8.34 (d, $J = 7.78$ Hz, 1 H), 9.81 (d, $J = 7.53$ Hz, 1 H). LCMS: $R_t = 0.90$ min, MS m/z = 372 $(M + H)^+$.

Synthesis of Compound 19 (GSK2801). Route 2:

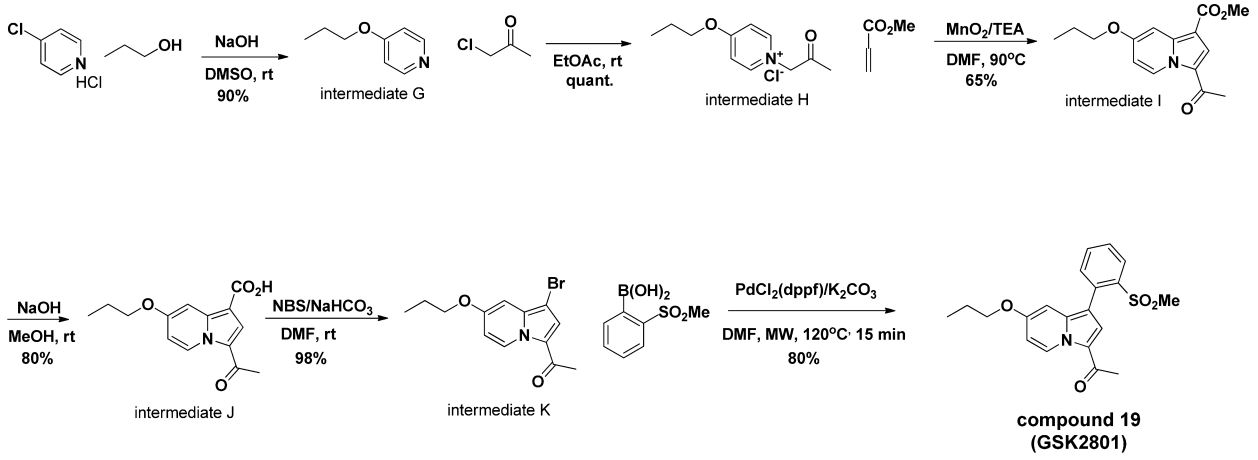

Synthesis of Compound ***19*** *(GSK2801) Intermediate G.* 4-Chloropyridine hydrochloride (10 g, 66.7 mmol) in dimethyl sulfoxide (DMSO) (10 mL) was treated with NaOH (2.93 g, 73.3 mmol). The mixture was stirred at ambient temperature for 30 min. To this mixture was added propan-1-ol (35.1 mL, 467 mmol) and then NaOH (2.93 g, 73.3 mmol). The mixture was stirred at 80 °C for 3 days. The mixture was allowed to

DOI: 10.1021/acs.jmedchem.5b00209
J. Med. Chem. 2016, 59, 1410−1424

cool to room temperature, treated with water, and extracted with EtOAc. The organics were washed with water and brine and then dried over Na_2SO_4. The filtrate was concentrated and dried to give 4-propoxypyridine (8.3 g, 60.5 mmol, 91% yield) as a yellow oil.

*Synthesis of Compound **19** (GSK2801) Intermediate H.* To a solution of 4-propoxypyridine (8.2 g, 59.8 mmol) in ethyl acetate (20 mL) was added 1-chloropropan-2-one (14.28 mL, 179 mmol). The mixture was stirred at ambient temperature overnight. The precipitated solid was filtered, washed with diethyl ether, and dried to give the indicated product quantitatively as a colorless solid.

*Synthesis of Compound **19** (GSK2801) Intermediate I.* To a suspension of 1-(2-oxopropyl)-4-propoxypyridin-1-ium chloride (6.03 g, 26.4 mmol) and manganese dioxide (9.17 g, 105 mmol) in DMF (30 mL) was added methyl acrylate (14.23 mL, 158 mmol) and TEA (4.41 mL, 31.6 mmol). The mixture was stirred at 90 °C for 3 h. The mixture was allowed to cool to room temperature, filtered through Celite, washed with EtOAc, and filtered. The combined filtrate was washed with water and brine, dried over Na_2SO_4, and filtered. The filtrate was concentrated, then purified by silica gel chromatography (0 to 60% EtOAc in heptane) to give methyl 3-acetyl-7-propoxyindolizine-1-carboxylate (5 g, 18.16 mmol, 68.9% yield) as a yellow solid. LCMS suggested that the product was 75% pure, and it was taken to the next step without further purification.

*Synthesis of Compound **19** (GSK2801) Intermediate J.* To a solution of methyl 3-acetyl-7-propoxyindolizine-1-carboxylate (3 g, 10.90 mmol) in methanol (15 mL), tetrahydrofuran (THF) (15.00 mL), and water (15.00 mL) was added 4 N NaOH (8.17 mL, 32.7 mmol). The mixture was stirred at ambient temperature for 3 days. The solution was concentrated and then acidified with 1 N HCl to pH = 1. The precipitated solid was filtered, washed with water, and dried to give 3-acetyl-7-propoxyindolizine-1-carboxylic acid (2.35 g, 8.99 mmol, 83% yield) as a yellow solid.

*Synthesis of Compound **19** (GSK2801) Intermediate K.* To a solution of 3-acetyl-7-propoxyindolizine-1-carboxylic acid (0.95 g, 3.64 mmol) in DMF (15 mL) was added sodium bicarbonate (0.916 g, 10.91 mmol) and then NBS (0.712 g, 4.00 mmol) portionwise at 0 °C. The cooling bath was removed, and the mixture was allowed to stir at ambient temperature for 1 h. The solution was treated with water and extracted with EtOAc. The combined organics were washed with water, then brine, and dried over Na_2SO_4 and filtered. The filtrate was concentrated to dryness to give 1-(1-bromo-7-propoxyindolizin-3-yl)ethanone (1.05 g, 3.55 mmol, 98% yield) as an off-white solid. The product was used in the next step without further purification.

Compound 19 (GSK2801). Nitrogen gas was bubbled through a mixture of 1-(1-bromo-7-propoxyindolizin-3-yl)ethanone (534 mg, 1.803 mmol), (2-(methylsulfonyl)phenyl)boronic acid (721 mg, 3.61 mmol), K_2CO_3 (748 mg, 5.41 mmol), and $PdCl_2$(dppf)−CH_2Cl_2 adduct (118 mg, 0.144 mmol) in DMF (7 mL) and water (0.5 mL) for 10 min. Then the mixture was irradiated in a sealed tube in the microwave (120 °C, 15 min).

The mixture was treated with EtOAc and filtered to remove solids. The filtrate was washed with water and brine, dried over Na_2SO_4, and filtered. The filtrate was concentrated, then purified with silica gel chromatography (0 to 50% EtOAc in heptane) to give 1-(1-(2-(methylsulfonyl)phenyl)-7-propoxyindolizin-3-yl)ethanone (535 mg, 1.442 mmol, 80% yield) as an off-white solid, which was identical to the GSK2801 prepared by Scheme 1 (above).

Synthesis of Inactive Control Compound 23 (GSK8573): 1-(1-(3-Methoxyphenyl)-7-propoxyindolizin-3-yl)ethanone. Compound **23** (GSK8573) was synthesized from intermediate K, which was made as described in the synthesis of probe compound 19 (GSK2801). Nitrogen gas was bubbled through a mixture of 1-(1-bromo-7-propoxyindolizin-3-yl)ethanone (544 mg, 1.837 mmol), (3-methoxyphenyl)boronic acid (419 mg, 2.76 mmol), K_2CO_3 (762 mg, 5.51 mmol), and $PdCl_2$(dppf)−CH_2Cl_2 adduct (120 mg, 0.147 mmol) in 1,4-dioxane (8 mL) and water (0.08 mL) and heated in a sealed tube in the microwave (100 °C, 6 min). The solid was filtered off and washed with EtOAc. The combined filtrate was concentrated and then purified with silica gel chromatography, eluting with 0 to 35% EtOAc in heptane to give 1-(1-(3-methoxyphenyl)-7-propoxyindolizin-3-yl)ethanone (364 mg, 1.126 mmol, 61.3% yield) as a yellow solid.

^{1}H NMR (400 MHz, DMSO-d_6) δ ppm 1.00 (t, J = 7.40 Hz, 3 H), 1.77 (q, J = 6.69 Hz, 2 H), 2.50 (s, 3H), 3.83 (s, 3 H), 4.07 (t, J = 6.40 Hz, 2 H), 6.84 (ddd, J = 18.95, 7.78, 2.38 Hz, 2 H), 7.17 (t, J = 2.64 Hz, 2 H), 7.23 (d, J = 7.78 Hz, 1 H), 7.33−7.43 (m, 1 H), 7.94 (s, 1 H), 9.69 (d, J = 7.78 Hz, 1 H). LCMS R_t = 0.97.

^{1}H NMR (400 MHz, methanol-d_4), δ ppm 1.00−1.17 (m, 3 H), 1.78−1.94 (m, 2 H), 2.56 (s, 3 H), 3.88 (s, 3 H), 4.05 (s, 2 H), 6.68−6.80 (m, 1 H), 6.85−6.95 (m, 1 H), 7.08−7.23 (m, 3 H), 7.33−7.46 (m, 1 H), 7.77 (s, 1 H), 9.68−9.81 (m, 1 H); LCMS: R_t = 1.06 min, MS m/z = 324 $(M + H)^+$.

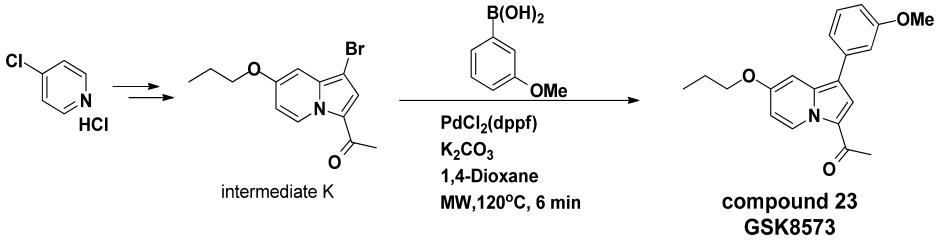

Example synthesis using alkyne route (Scheme 1a in main text). Compound **15**: 1-(1-(2-(hydroxymethyl)phenyl)-7-morpholinoindolizin-3-yl)ethanone.

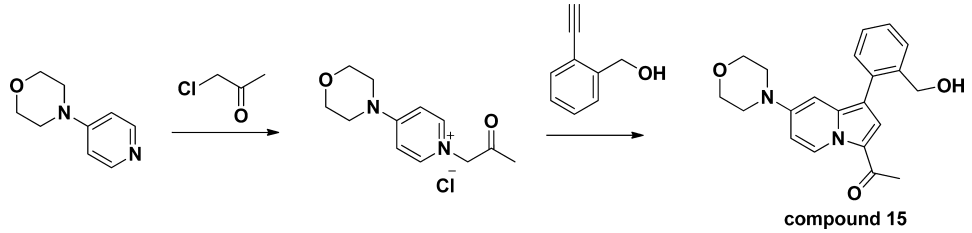

4-Morpholino-1-(2-oxopropyl)pyridin-1-ium chloride: A mixture of 4-(pyridin-4-yl)morpholine (2.037 mL, 12.18 mmol) and 1-chloropropan-2-one (4.90 mL, 60.9 mmol) was heated at 85 °C for 2 h. The precipitated solid was filtered and washed with ethyl acetate and then diethyl ether to give 4-morpholino-1-(2-oxopropyl)pyridin-1-ium chloride (3.1 g, 99%). ^{1}H NMR (400 MHz, DMSO-d_6) δ ppm 2.26 (s, 3 H), 3.74 (dd, J = 14.49, 4.50 Hz, 8 H), 5.35 (s, 2 H), 7.32 (d, J = 7.44 Hz, 2 H), 8.17 (d, J = 7.44 Hz, 2 H).

Compound 15: 1-(1-(2-(Hydroxymethyl)phenyl)-7-morpholinoindolizin-3-yl)ethanoneA slurry of 4-morpholino-1-(2-oxopropyl)-pyridin-1-ium chloride (291 mg, 1.135 mmol), (2-ethynylphenyl)-methanol (50 mg, 0.378 mmol), and K_2CO_3 (261 mg, 1.892 mmol) in

DOI: 10.1021/acs.jmedchem.5b00209
J. Med. Chem. 2016, 59, 1410−1424

DMF was irradiated in microwave at 120 °C for 30 min. The product was purified with reverse phase HPLC (10−100% acetonitrile in water for 6 min and 100% acetonitrile for 1 min, with 0.05% TFA as additive) to give 1-(1-(2-(hydroxymethyl)phenyl)-7-morpholinoindolizin-3-yl)-ethanone (18 mg, 13.56%). ^{1}H NMR (400 MHz, DMSO-d_6) δ ppm 2.43 (s, 3 H), 3.20 (br. s., 4 H), 3.72 (br. s., 4 H), 4.44 (s, 2 H), 6.55 (s, 1 H), 7.04 (s, 1 H), 7.28−7.43 (m, 3 H), 7.61 (br. s., 1 H), 7.69 (s, 1 H), 9.63 (d, J = 7.78 Hz, 1 H). LCMS: R_t = 0.71 min, MS m/z = 351 $(M + H)^+$.

Compound 2 was prepared in a manner similar to that described for compound **15**. ^{1}H NMR (400 MHz, DMSO-d_6) δ ppm 2.50 (s, 3 H), 3.39 (t, J = 4.50 Hz, 4 H), 3.82 (t, J = 4.60 Hz, 4 H), 7.05−7.18 (m, 1 H), 7.23−7.34 (m, 1 H), 8.00 (d, J = 15.27 Hz, 3 H), 8.32 (s, 1 H), 8.64 (d, J = 4.50 Hz, 1 H), 9.66 (d, J = 7.83 Hz, 1 H). LCMS: R_t = 0.62 min, MS m/z = 322 $(M + H)^+$.

Example synthesis of indolizine compound **3**: 1-(1-(3-methoxyphenyl)-indolizin-3-yl)ethanone.

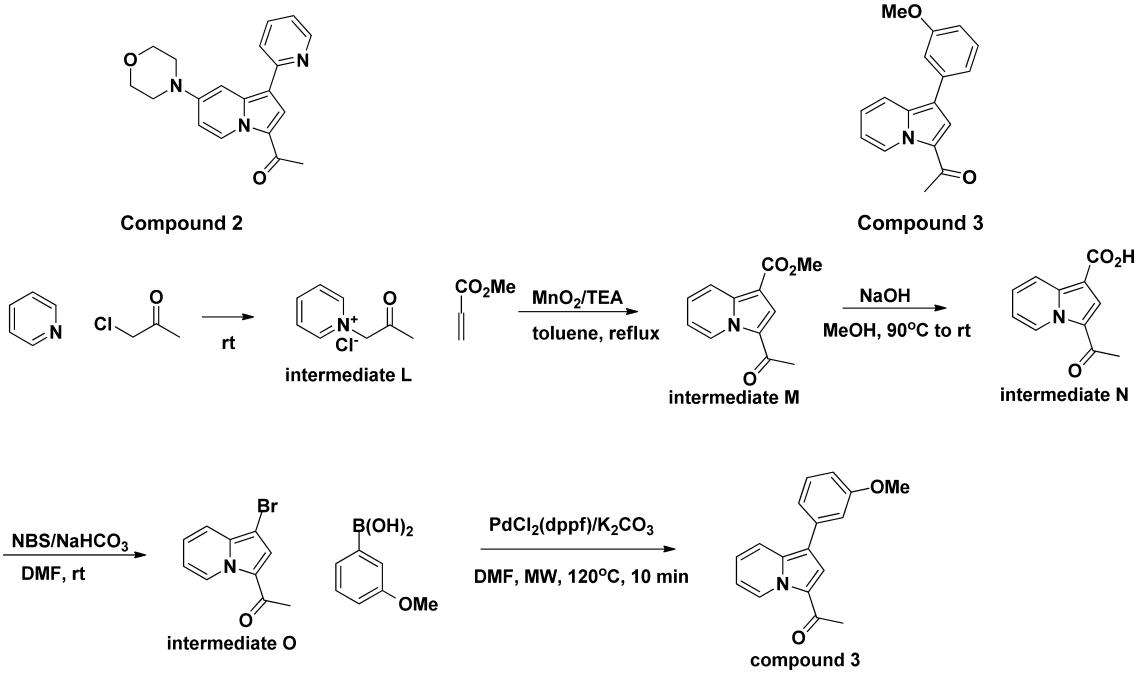

Intermediate L: (1-(2-Oxopropyl)pyridin-1-ium chloride). A mixture of pyridine (10 mL, 124 mmol) and 1-chloropropan-2-one (4.3 mL, 53.4 mmol) was heated at 85 °C for 1 h. The solid was filtered and washed with diethyl ether to give 1-(2-oxopropyl)-pyridin-1-ium chloride (9 g, 52.4 mmol, 98% yield). The product was used in the next step without further purification. ^{1}H NMR (400 MHz, DMSO-d_6) δ ppm 2.35 (s, 3 H), 5.93 (s, 2 H), 8.25 (t, J = 6.95 Hz, 2 H), 8.71 (t, J = 7.73 Hz, 1 H), 8.99 (d, J = 5.87 Hz, 2 H).

Intermediate M: (Methyl 3-acetylindolizine-1-carboxylate). A suspension of 1-(2-oxopropyl)pyridin-1-ium chloride (5 g, 29.1 mmol), methyl acrylate (21.81 mL, 291 mmol), manganese dioxide (20.26 g, 233 mmol), and TEA (6.09 mL, 43.7 mmol) in toluene (50 mL) was refluxed for 2 h. The suspension was filtered over Celite and washed with acetone, and the filtrate was concentrated to dryness to give methyl 3-acetylindolizine-1-carboxylate (5.6 g, 25.8 mmol, 88% yield). The product was used in the next step without further purification. LCMS: R_t = 0.71 min, MS m/z = 218 $(M + H)^+$.

Intermediate N: (3-Acetylindolizine-1-carboxylic acid). A solution of methyl 3-acetylindolizine-1-carboxylate (7 g, 32.2 mmol) and NaOH (4M, 81 mL, 322 mmol) in methanol (100 mL) was stirred at 90 °C for 3 h and then at rt overnight. The solution was concentrated and distributed between DCM and water. The aqueous phase was acidified with 6 N HCl, and the precipitate was filtered, washed with water, and dried to give 3-acetylindolizine-1-carboxylic acid (4.3 g, 21.16 mmol, 65.7% yield). The product was used in the next step without further purification. ^{1}H NMR (400 MHz, Chloroform-d) δ ppm 2.59 (s, 3 H), 6.97 (t, J = 6.85 Hz, 1 H), 7.22−7.31 (m, 2 H), 7.50−7.70 (m, 2 H), 9.90 (d, J = 7.24 Hz, 1 H). LCMS: R_t = 0.55 min, MS m/z = 204 $(M + H)^+$.

Intermediate O: (1-(1-Bromoindolizin-3-yl)ethanone). To a solution of 3-acetylindolizine-1-carboxylic acid (2 g, 9.84 mmol) in DMF (15 mL) was added sodium bicarbonate (2.481 g, 29.5 mmol) and then NBS (1.839 g, 10.33 mmol) portion-wise. The mixture was stirred at rt for 20 min. The mixture was distributed between water and EtOAc, and the aqueous layer further extracted with EtOAc. The combined organics were washed with water and brine, dried over Na_2SO_4, and filtered. The filtrate was concentrated. The product was purified on the Biotage eluting with EtOAc in hexanes (0−30%) to give 1-(1-bromoindolizin-3-yl)ethanone (2.1 g, 8.82 mmol, 90% yield) as a green solid. ^{1}H NMR (400 MHz, DMSO-d_6) δ ppm 2.47−2.54 (m, 3 H), 7.12 (td, J = 6.90, 1.25 Hz, 1 H), 7.39 (ddd, J = 8.78, 6.78, 1.00 Hz, 1 H), 7.55−7.70 (m, 1 H), 7.97 (s, 1 H), 9.74 (d, J = 7.03 Hz, 1 H). LCMS: R_t = 0.83 min, MS m/z = 238 $(M + H)^+$.

Compound 3: (1-(1-(3-Methoxyphenyl)indolizin-3-yl)ethanone). A mixture of 1-(1-bromoindolizin-3-yl)ethanone (65 mg, 0.273 mmol), (3-methoxyphenyl)boronic acid (49.8 mg, 0.328 mmol), K_2CO_3 (113 mg, 0.819 mmol), and $PdCl_2$(dppf)−CH_2Cl_2 adduct (15.61 mg, 0.019 mmol) in DMF (3 mL) and 4 drops of water were irradiated in the microwave at 120 °C for 10 min. The product was purified with reverse phase HPLC (50−100% acetonitrile in water for 6 min and 100% acetonitrile for 1 min, with 0.05% TFA as additive) to give 1-(1-(3-methoxyphenyl)indolizin-3-yl)ethanone (32 mg, 0.121 mmol, 44% yield). ^{1}H NMR (400 MHz, methanol-d_4) δ ppm 2.61 (s, 3 H), 3.88 (s, 3 H), 6.91 (dd, J = 7.91, 2.13 Hz, 1 H), 7.02 (td, J = 6.90, 1.00 Hz, 1 H), 7.13−7.17 (m, 1 H), 7.20 (d, J = 7.78 Hz, 1 H), 7.31 (ddd, J = 8.91, 6.78, 0.88 Hz, 1 H), 7.35−7.43 (m, 1 H), 7.83 (s, 1 H), 7.91 (d, J = 8.78 Hz, 1 H), 9.86 (d, J = 7.28 Hz, 1 H). LCMS: R_t = 1.18 min, MS m/z = 266 $(M + H)^+$.

Compound 4, 1-(1-(Thiophen-2-yl)indolizin-3-yl)ethanone, was prepared in a manner similar to that described for compound **3**, using intermediate O. The Suzuki reaction was performed using thiophen-2-yl-boronic acid, $PdCl_2$(dppf)−CH_2Cl_2 adduct as catalyst and heating in the microwave at 120 °C for 10 min (yield = 34%). ^{1}H NMR (400 MHz, methanol-d_4) δ ppm 2.58 (s, 3 H), 7.01 (t, J = 6.85 Hz, 1 H), 7.13 (dd, J = 4.89, 3.72 Hz, 1 H), 7.26−7.41 (m, 3 H), 7.83 (s, 1 H), 7.99

DOI: 10.1021/acs.jmedchem.5b00209
J. Med. Chem. 2016, 59, 1410−1424

(d, J = 8.81 Hz, 1 H), 9.82 (d, J = 7.05 Hz, 1 H). LCMS: R_t = 0.87 min, MS m/z = 242 $(M + H)^+$.

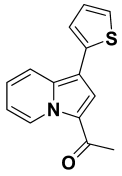

Compound 4

Compound 5, 1-(1-(2-hydroxyphenyl)indolizin-3-yl)ethanone, was prepared in a manner similar to that described for compound **3** using intermediate O. The Suzuki reaction was performed using (2-hydroxyphenyl)boronic acid, $PdCl_2(dppf)-CH_2Cl_2$ adduct as catalyst, and heating in the microwave at 120 °C for 10 min (yield = 43%). ^{1}H NMR (400 MHz, DMSO-d_6) δ ppm 2.56 (s, 3 H), 6.93 (t, J = 7.34 Hz, 1 H), 7.01 (d, J = 7.83 Hz, 1 H), 7.08 (t, J = 6.56 Hz, 1 H), 7.18−7.24 (m, 1 H), 7.25−7.32 (m, 1 H), 7.38 (d, J = 6.46 Hz, 1 H), 7.64 (d, J = 8.81 Hz, 1 H), 7.85 (s, 1 H), 9.54 (s, 1 H), 9.81 (d, J = 7.05 Hz, 1 H). LCMS: R_t = 0.85 min, MS m/z = 252 $(M + H)^+$.

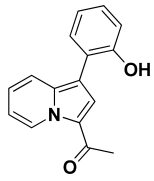

Compound 5

Compound 6, 1-(1-(3-hydroxyphenyl)indolizin-3-yl)ethanone, was prepared in a manner similar to that described for compound **3** using intermediate O. The Suzuki reaction was performed using (3-hydroxyphenyl)boronic acid, $PdCl_2(dppf)-CH_2Cl_2$ adduct as catalyst, and heating in the microwave at 120 °C for 20 min (yield = 37%). ^{1}H NMR (400 MHz, $CDCl_3$) δ 9.96 (d, 1H, J = 6.7 Hz), 7.91 (d, 1H, J = 8.6 Hz), 7.66 (s, 1H), 7.38−7.13 (m, 3H), 6.98−6.85 (m, 2H), 5.25 (s, 1H), 2.66 (s, 3H). LRMS (ESI-TOF) $[M + H]^+$ m/z calcd for $C_{16}H_{13}NO_2H^+$, 252.1; found, 252.1.

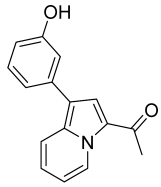

Compound 6

Compound 7, 1-(1-(2-(hydroxymethyl)phenyl)indolizin-3-yl)-ethanone, was prepared using the alkyne route in a manner similar to that described for compound **15**. ^{1}H NMR (500 MHz, $CDCl_3$) δ 9.96 (d,1H, J = 7 Hz), 7.68−7.66 (m, 2H), 7.50−7.45 (m, 4H), 7.31 (s, 1H), 7.19 (t, 1H, J = 7.6 Hz), 6.97 (t, 1H, J = 7.6 Hz), 4.69 (s, 2H), 2.64 (s, 3H). LRMS (ESI-TOF) $[M + H]^+$ m/z calcd for $C_{17}H_{15}NO_2H^+$, 266.1; found, 266.1.

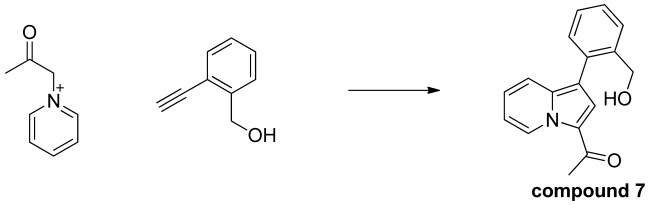

compound 7

Compound 8, 3-(3-acetylindolizin-1-yl)benzamide, was prepared in a manner similar to that described for compound **3** using intermediate O. The Suzuki reaction was performed using (3-carbamoylphenyl)-boronic acid, $PdCl_2(dppf)-CH_2Cl_2$ adduct as catalyst, and heating in the microwave at 120 °C for 10 min (yield = 56%). ^{1}H NMR (400 MHz, DMSO-d_6) δ ppm 2.62 (s, 3 H), 7.15 (t, J = 6.75 Hz, 1 H), 7.36−7.44 (m, 1 H), 7.49 (br. s., 1 H), 7.56−7.63 (m, 1 H), 7.85 (t, J = 8.81 Hz, 2 H), 8.05 (d, J = 9.00 Hz, 1 H), 8.13 (br. s, 2 H), 8.17 (s, 1 H), 9.85 (d, J = 7.24 Hz, 1 H). LCMS: R_t = 0.68 min, MS m/z = 279 $(M + H)^+$.

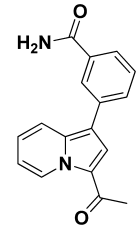

Compound 8

Compound 9, 1-(1-(2-(hydroxymethyl)-4-methoxyphenyl)-indolizin-3-yl)ethanone, was prepared in a manner similar to that described for compound **3** using intermediate O. The Suzuki reaction was performed using (2-(hydroxymethyl)-4-methoxyphenyl)boronic acid, $PdCl_2(dppf)-CH_2Cl_2$ adduct as catalyst, and heating in the microwave at 120 °C for 10 min (yield = 11%). ^{1}H NMR (400 MHz, chloroform-d) δ ppm 2.56−2.67 (m, 3 H), 3.94 (s, 3 H), 4.65 (s, 2 H), 6.92−7.01 (m, 2 H), 7.14−7.21 (m, 1 H), 7.23 (d, J = 2.15 Hz, 1 H), 7.34 (d, J = 8.42 Hz, 1 H), 7.44 (d, J = 9.00 Hz, 1 H), 7.59 (s, 1 H), 9.95 (d, J = 7.05 Hz, 1 H). LCMS: R_t = 0.79 min, MS m/z = 296 $(M + H)^+$.

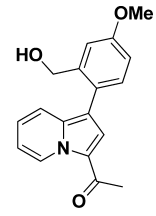

Compound 9

Compound 10, 1-(1-(4-(hydroxymethyl)phenyl)indolizin-3-yl)-ethanone, was prepared in a manner similar to that described for compound **3** using intermediate O. The Suzuki reaction was performed using (4-(hydroxymethyl)phenyl)boronic acid, $PdCl_2(dppf)-CH_2Cl_2$ adduct as catalyst, and heating in the microwave at 120 °C for 10 min (yield = 11%). ^{1}H NMR (400 MHz, DMSO-d_6) δ ppm 2.60 (s, 3 H), 4.58 (d, J = 4.11 Hz, 2 H), 5.24 (br. s., 1 H), 7.12 (t, J = 6.66 Hz, 1 H), 7.32−7.41 (m, 1 H), 7.46 (d, J = 7.83 Hz, 2 H), 7.67 (d, J = 8.03 Hz, 2 H), 7.99 (d, J = 9.00 Hz, 1 H), 8.03 (s, 1 H), 9.84 (d, J = 7.05 Hz, 1 H). LCMS: R_t = 0.78 min, MS m/z = 266 $(M + H)^+$.

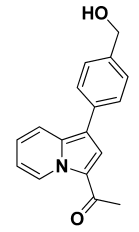

Compound 10

Compound 11, 1-(1-(4-(dimethylamino)phenyl)indolizin-3-yl)-ethanone, was prepared in a manner similar to that described for compound **3** using intermediate O. ^{1}H NMR (400 MHz, $CDCl_3$) δ 9.92 (d, 1H, J = 7 Hz), 7.83 (d, 1H, J = 9 Hz), 7.58 (s, 1H), 7.48 (d, 2H, J = 7.5 Hz), 7.17−7.16 (m, 1H), 6.90−6.86 (m, 3H), 3.03 (s, 6H), 2.62 (s, 3H). LRMS (ESI-TOF) $[M + H]^+$ m/z calcd for $C_{18}H_{18}N_2OH^+$, 279.2; found, 279.3.

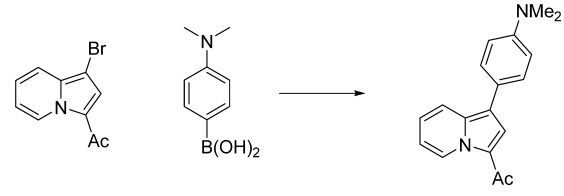

DOI: 10.1021/acs.jmedchem.5b00209
J. Med. Chem. 2016, 59, 1410−1424

Compound 12, 1-(1-(2-(methylsulfonyl)phenyl)indolizin-3-yl)-ethanone, was prepared in a manner similar to that described for compound **3** using intermediate O. ^{1}H NMR (400 MHz, DMSO-d_6) δ ppm 2.55 (s, 3 H), 2.85 (s, 3H), 7.14 (t, J = 6.56 Hz, 1 H), 7.27−7.35 (m, 1 H), 7.37−7.43 (m, 1 H), 7.58 (d, J = 7.05 Hz, 1 H), 7.71−7.78 (m, 1 H), 7.80−7.87 (m, 1 H), 7.96 (s, 1 H), 8.20 (d, J = 7.83 Hz, 1 H), 9.81 (d, J = 7.05 Hz, 1 H). LCMS: R_t = 0.79 min, MS m/z = 314 $(M + H)^+$.

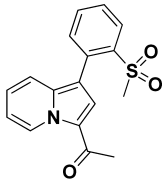

Compound 12

Compound 13, 1-(1-(2-(hydroxymethyl)phenyl)-7-methylindolizin-3-yl)ethanone, was prepared in a manner similar to that described for compound **3**. ^{1}H NMR (400 MHz, DMSO-d_6) δ ppm 2.34 (s, 3 H), 2.50 (s, 3 H), 4.44 (s, 2 H), 5.10 (br. s., 1 H), 6.94 (dd, J = 7.15, 1.13 Hz, 1 H), 7.26 (s, 1 H), 7.31−7.44 (m, 3 H), 7.63 (d, J = 7.53 Hz, 1 H), 7.80 (s, 1 H), 9.69 (d, J = 7.28 Hz, 1 H). LCMS: R_t = 0.79 min, MS m/z = 280 $(M + H)^+$.

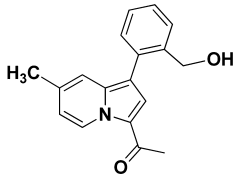

Compound 13

Compound 14, 1-(1-(2-(hydroxymethyl)phenyl)-7-methoxyindolizin-3-yl)ethanone, was prepared in a manner similar to that described for compound **3**. ^{1}H NMR (400 MHz, DMSO-d_6) δ ppm 2.47 (s, 3 H), 3.79 (s, 3 H), 4.45 (s, 2 H), 6.76 (s, 1 H), 6.80 (d, J = 7.53 Hz, 1 H), 7.30−7.44 (m, 3 H), 7.63 (d, J = 7.28 Hz, 1 H), 7.78 (s, 1 H), 9.68 (d, J = 7.53 Hz, 1 H). LCMS: R_t = 0.80 min, MS m/z = 296 $(M + H)^+$.

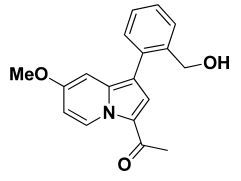

Compound 14

Compound 16, 3-acetyl-1-(2-(hydroxymethyl)phenyl)indolizine-7-carboxamide, was prepared in a manner similar to that described for compound **3**. ^{1}H NMR (400 MHz, DMSO-d_6) δ ppm 2.60 (s, 3 H), 4.48 (s, 2 H), 7.38−7.59 (m, 5 H), 7.69 (d, J = 7.44 Hz, 1 H), 7.97 (s, 1 H), 8.03 (s, 1 H), 8.23 (br. s., 1 H), 9.77 (d, J = 7.24 Hz, 1 H). LCMS: R_t = 0.64 min, MS m/z = 309 $(M + H)^+$.

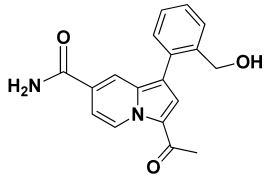

Compound 16

Compound 17, 1-(1-(2-(hydroxymethyl)phenyl)-7-phenoxyindolizin-3-yl)ethanone, was prepared in a manner similar to that described for compound **3**. ^{1}H NMR (400 MHz, DMSO-d_6) δ ppm 2.50 (s, 3 H), 4.41 (d, J = 5.27 Hz, 2 H), 5.11 (s, 1 H), 6.70 (s, 1 H), 6.95 (d, J = 7.78 Hz, 1 H), 7.13−7.37 (m, 6 H), 7.44 (t, J = 7.78 Hz, 2 H), 7.57 (d, J = 7.53 Hz, 1 H), 7.85 (s, 1 H), 9.80 (d, J = 7.53 Hz, 1 H). LCMS: R_t = 0.92 min, MS m/z = 358 $(M + H)^+$.

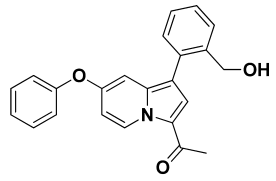

Compound 17

Compound 18, *tert*-butyl ((3-acetyl-1-(2-(methylsulfonyl)phenyl)-indolizin-7-yl)methyl)carbamate, was prepared in a manner similar to that described for compound **3**. ^{1}H NMR (400 MHz, methanol-d_4) δ ppm 1.40 (s, 9 H), 2.58 (s, 3 H), 2.70 (s, 3 H), 4.25 (s, 2 H), 6.99 (d, J = 7.28 Hz, 1 H), 7.24 (s, 1 H), 7.57 (d, J = 7.28 Hz, 1 H), 7.66−7.73 (m, 1 H), 7.75−7.83 (m, 1 H), 7.92 (s, 1 H), 8.27 (d, J = 8.03 Hz, 1 H), 9.80 (d, J = 7.28 Hz, 1 H). LCMS: R_t = 0.82 min, MS m/z = 443 $(M + H)^+$.

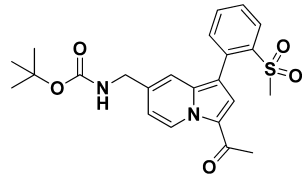

Compound 18

Compound 20, 1-(1-(2-(methylsulfonyl)phenyl)-7-phenoxyindolizin-3-yl)ethanone, was prepared in a manner similar to that described for compound **3**. ^{1}H NMR (400 MHz, chloroform-d) δ ppm 2.62 (s, 3 H), 2.70 (s, 3 H), 6.78 (dd, J = 7.73, 2.45 Hz, 1 H), 6.85 (d, J = 2.35 Hz, 1 H), 7.11 (d, J = 7.83 Hz, 2 H), 7.20−7.27 (m, 1 H), 7.39−7.51 (m, 3 H), 7.55−7.62 (m, 1 H), 7.64−7.72 (m, 1 H), 7.92 (s, 1 H), 8.32 (d, J = 7.63 Hz, 1 H), 9.95 (d, J = 7.63 Hz, 1 H). LCMS: R_t = 0.92 min, MS m/z = 406 $(M + H)^+$.

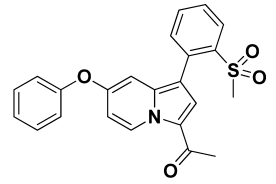

Compound 20

Compound 21, 1-(7-methoxy-1-(2-(methylsulfonyl)phenyl)-indolizin-3-yl)ethanone, was prepared in a manner similar to that described for compound **3**. ^{1}H NMR (400 MHz, DMSO-d_6) δ ppm 2.46 (s, 3 H), 2.82 (s, 3 H), 3.76 (s, 3 H), 6.65 (d, J = 2.51 Hz, 1 H), 6.83 (dd, J = 7.65, 2.38 Hz, 1 H), 7.57 (d, J = 7.53 Hz, 1 H), 7.66−7.74 (m, 1 H), 7.76−7.85 (m, 2 H), 8.17 (d, J = 7.78 Hz, 1 H), 9.67 (d, J = 7.78 Hz, 1 H). LCMS: R_t = 0.80 min, MS m/z = 344 $(M + H)^+$.

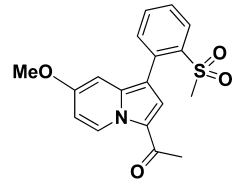

Compound 21

Compound 22, 1-(7-methyl-1-(2-(methylsulfonyl)phenyl)indolizin-3-yl)ethanone, was prepared in a manner similar to that described for compound **3**. ^{1}H NMR (400 MHz, DMSO-d_6) δ ppm 2.32 (s, 3 H), 2.49 (s, 3 H), 2.81 (s, 3 H), 6.97 (dd, J = 7.40, 1.38 Hz, 1 H), 7.16 (s, 1 H), 7.54 (d, J = 7.53 Hz, 1 H), 7.67−7.74 (m, 1 H), 7.77−7.83 (m, 1 H), 7.87 (s, 1 H), 8.16 (d, J = 8.03 Hz, 1 H), 9.69 (d, J = 7.28 Hz, 1 H). LCMS: R_t = 0.82 min, MS m/z =328 $(M + H)^+$.

DOI: 10.1021/acs.jmedchem.5b00209
J. Med. Chem. 2016, 59, 1410−1424

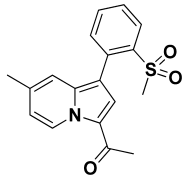

Compound 22

The cocrystal structures reported in this study have been deposited to the protein data bank under accession codes 4IR3, 4IR4, 4IR5, 4IR6 and 4RVR.

■ ASSOCIATED CONTENT

Supporting Information

Additional method descriptions, a crystallographic data collection and refinement table, and supplemental figures showing the electron density around the cocrystallized ligands. This material is available free of charge via the Internet at http://pubs.acs.org.

■ AUTHOR INFORMATION

Corresponding Authors

*E-mail: Knapp@pharmchem.uni-frankfurt.de. Phone: +49 69 79 82 98 71.

*E-mail: davidhdrewry@gmail.com. Phone: +1 919 602 1327.

Author Contributions

○These authors contributed equally to this work.

Notes

The authors declare no competing financial interest.

■ ACKNOWLEDGMENTS

The SGC is a registered charity (number 1097737) that receives funds from AbbVie, Bayer Pharma AG, Boehringer Ingelheim, the Canada Foundation for Innovation, Genome Canada, GlaxoSmithKline, Janssen, Lilly Canada, the Novartis Research Foundation, the Ontario Ministry of Economic Development and Innovation, Pfizer, Takeda, and the Wellcome Trust [092809/Z/10/Z].

■ ABBREVIATIONS USED

BAZ2A, bromodomain adjacent to zinc finger domain protein 2A; BAZ2B, bromodomain adjacent to zinc finger domain protein 2B; B-ALL, B cell acute lymphoblastic leukemia; DMF, dimethylformamide; PHD, plant homology domain; BET, bromodomain and extraterminal; ISWI, imitation switch chromatin remodeling complexes; NoRC, nucleolar remodeling complex; FRAP, fluorescent recovery after photobleaching; SEM, standard error of the mean

■ REFERENCES

(1) Filippakopoulos, P.; Knapp, S. The bromodomain interaction module. *FEBS Lett.* **2012**, *586*, 2692−2704.

(2) Filippakopoulos, P.; Picaud, S.; Mangos, M.; Keates, T.; Lambert, J. P.; Barsyte-Lovejoy, D.; Felletar, I.; Volkmer, R.; Muller, S.; Pawson, T.; Gingras, A. C.; Arrowsmith, C. H.; Knapp, S. Histone recognition and large-scale structural analysis of the human bromodomain family. *Cell* **2012**, *149*, 214−231.

(3) Kouzarides, T. Acetylation: a regulatory modification to rival phosphorylation? *EMBO J.* **2000**, *19*, 1176−1179.

(4) Filippakopoulos, P.; Knapp, S. Targeting bromodomains: epigenetic readers of lysine acetylation. *Nat. Rev. Drug Discovery* **2014**, *13*, 337−356.

(5) Muller, S.; Filippakopoulos, P.; Knapp, S. Bromodomains as therapeutic targets. *Expert Rev. Mol. Med.* **2011**, *13*, e29.

(6) Knapp, S.; Weinmann, H. Small-molecule modulators for epigenetics targets. *ChemMedChem* **2013**, *11*, 1885−1891.

(7) Gallenkamp, D.; Gelato, K. A.; Haendler, B.; Weinmann, H. Bromodomains and their pharmacological inhibitors. *ChemMedChem* **2014**, *9*, 438−464.

(8) Zhao, Y.; Yang, C. Y.; Wang, S. The making of I-BET762, a BET bromodomain inhibitor now in clinical development. *J. Med. Chem.* **2013**, *56*, 7498−7500.

(9) Garnier, J. M.; Sharp, P. P.; Burns, C. J. BET bromodomain inhibitors: a patent review. *Expert Opin. Ther. Pat.* **2014**, *24*, 185−199.

(10) Ember, S. W.; Zhu, J. Y.; Olesen, S. H.; Martin, M. P.; Becker, A.; Berndt, N.; Georg, G. I.; Schonbrunn, E. Acetyl-lysine binding site of bromodomain-containing protein 4 (BRD4) interacts with diverse kinase inhibitors. *ACS Chem. Biol.* **2014**, *9*, 1160−1171.

(11) Dittmann, A.; Werner, T.; Chung, C. W.; Savitski, M. M.; Falth Savitski, M.; Grandi, P.; Hopf, C.; Lindon, M.; Neubauer, G.; Prinjha, R. K.; Bantscheff, M.; Drewes, G. The commonly used PI3-kinase probe LY294002 is an inhibitor of BET bromodomains. *ACS Chem. Biol.* **2014**, *9*, 495−502.

(12) Ciceri, P.; Muller, S.; O'Mahony, A.; Fedorov, O.; Filippakopoulos, P.; Hunt, J. P.; Lasater, E. A.; Pallares, G.; Picaud, S.; Wells, C.; Martin, S.; Wodicka, L. M.; Shah, N. P.; Treiber, D. K.; Knapp, S. Dual kinase-bromodomain inhibitors for rationally designed polypharmacology. *Nat. Chem. Biol.* **2014**, *10*, 305−312.

(13) Filippakopoulos, P.; Qi, J.; Picaud, S.; Shen, Y.; Smith, W. B.; Fedorov, O.; Morse, E. M.; Keates, T.; Hickman, T. T.; Felletar, I.; Philpott, M.; Munro, S.; McKeown, M. R.; Wang, Y.; Christie, A. L.; West, N.; Cameron, M. J.; Schwartz, B.; Heightman, T. D.; La Thangue, N.; French, C. A.; Wiest, O.; Kung, A. L.; Knapp, S.; Bradner, J. E. Selective inhibition of BET bromodomains. *Nature* **2010**, *468*, 1067−1073.

(14) Muller, S.; Knapp, S. Discovery of BET bromodomain inhibitors and their role in target validation. *MedChemComm* **2014**, *5*, 288−296.

(15) Picaud, S.; Da Costa, D.; Thanasopoulou, A.; Filippakopoulos, P.; Fish, P. V.; Philpott, M.; Fedorov, O.; Brennan, P.; Bunnage, M. E.; Owen, D. R.; Bradner, J. E.; Taniere, P.; O'Sullivan, B.; Muller, S.; Schwaller, J.; Stankovic, T.; Knapp, S. PFI-1, a highly selective protein interaction inhibitor, targeting BET bromodomains. *Cancer Res.* **2013**, *73*, 3336−3346.

(16) Mirguet, O.; Gosmini, R.; Toum, J.; Clement, C. A.; Barnathan, M.; Brusq, J. M.; Mordaunt, J. E.; Grimes, R. M.; Crowe, M.; Pineau, O.; Ajakane, M.; Daugan, A.; Jeffrey, P.; Cutler, L.; Haynes, A. C.; Smithers, N. N.; Chung, C. W.; Bamborough, P.; Uings, I. J.; Lewis, A.; Witherington, J.; Parr, N.; Prinjha, R. K.; Nicodeme, E. Discovery of epigenetic regulator I-BET762: lead optimization to afford a clinical candidate inhibitor of the BET bromodomains. *J. Med. Chem.* **2013**, *56*, 7501−7515.

(17) McNeill, E. RVX-208, a stimulator of apolipoprotein AI gene expression for the treatment of cardiovascular diseases. *Curr. Opin. Invest. Drugs* **2010**, *11*, 357−364.

(18) Mirguet, O.; Lamotte, Y.; Donche, F.; Toum, J.; Gellibert, F.; Bouillot, A.; Gosmini, R.; Nguyen, V. L.; Delannee, D.; Seal, J.; Blandel, F.; Boullay, A. B.; Boursier, E.; Martin, S.; Brusq, J. M.; Krysa, G.; Riou, A.; Tellier, R.; Costaz, A.; Huet, P.; Dudit, Y.; Trottet, L.; Kirilovsky, J.; Nicodeme, E. From ApoA1 upregulation to BET family bromodomain inhibition: discovery of I-BET151. *Bioorg. Med. Chem. Lett.* **2012**, *22*, 2963−2967.

(19) Filippakopoulos, P.; Picaud, S.; Fedorov, O.; Keller, M.; Wrobel, M.; Morgenstern, O.; Bracher, F.; Knapp, S. Benzodiazepines and benzotriazepines as protein interaction inhibitors targeting bromodomains of the BET family. *Bioorg. Med. Chem.* **2012**, *20*, 1878−1886.

(20) Seal, J.; Lamotte, Y.; Donche, F.; Bouillot, A.; Mirguet, O.; Gellibert, F.; Nicodeme, E.; Krysa, G.; Kirilovsky, J.; Beinke, S.; McCleary, S.; Rioja, I.; Bamborough, P.; Chung, C. W.; Gordon, L.; Lewis, T.; Walker, A. L.; Cutler, L.; Lugo, D.; Wilson, D. M.; Witherington, J.; Lee, K.; Prinjha, R. K. Identification of a novel series of BET family bromodomain inhibitors: binding mode and profile of I-

DOI: 10.1021/acs.jmedchem.5b00209
J. Med. Chem. 2016, 59, 1410−1424

BET151 (GSK1210151A). *Bioorg. Med. Chem. Lett.* **2012**, *22*, 2968−2972.
(21) Drouin, L.; McGrath, S.; Vidler, L. R.; Chaikuad, A.; Monteiro, O.; Tallant, C.; Philpott, M.; Rogers, C.; Fedorov, O.; Liu, M.; Akhtar, W.; Hayes, A.; Raynaud, F.; Muller, S.; Knapp, S.; Hoelder, S. Structure enabled design of BAZ2-ICR, a chemical probe targeting the bromodomains of BAZ2A and BAZ2B. *J. Med. Chem.* **2015**, *58*, 2553−2559.
(22) Jones, M. H.; Hamana, N.; Nezu, J.; Shimane, M. A novel family of bromodomain genes. *Genomics* **2000**, *63*, 40−45.
(23) Strohner, R.; Nemeth, A.; Jansa, P.; Hofmann-Rohrer, U.; Santoro, R.; Langst, G.; Grummt, I. NoRC−a novel member of mammalian ISWI-containing chromatin remodeling machines. *EMBO J.* **2001**, *20*, 4892−4900.
(24) Mayer, C.; Neubert, M.; Grummt, I. The structure of NoRC-associated RNA is crucial for targeting the chromatin remodelling complex NoRC to the nucleolus. *EMBO Rep.* **2008**, *9*, 774−780.
(25) Mayer, C.; Schmitz, K. M.; Li, J.; Grummt, I.; Santoro, R. Intergenic transcripts regulate the epigenetic state of rRNA genes. *Mol. Cell* **2006**, *22*, 351−361.
(26) Zhou, Y.; Grummt, I. The PHD finger/bromodomain of NoRC interacts with acetylated histone H4K16 and is sufficient for rDNA silencing. *Curr. Biol.* **2005**, *15*, 1434−1438.
(27) Gu, L.; Frommel, S. C.; Oakes, C. C.; Simon, R.; Grupp, K.; Gerig, C. Y.; Bar, D.; Robinson, M. D.; Baer, C.; Weiss, M.; Gu, Z.; Schapira, M.; Kuner, R.; Sultmann, H.; Provenzano, M.; Cancer, I. P. o. E. O. P.; Yaspo, M. L.; Brors, B.; Korbel, J.; Schlomm, T.; Sauter, G.; Eils, R.; Plass, C.; Santoro, R. BAZ2A (TIP5) is involved in epigenetic alterations in prostate cancer and its overexpression predicts disease recurrence. *Nat. Genet.* **2015**, *47*, 22−30.
(28) Arking, D. E.; Junttila, M. J.; Goyette, P.; Huertas-Vazquez, A.; Eijgelsheim, M.; Blom, M. T.; Newton-Cheh, C.; Reinier, K.; Teodorescu, C.; Uy-Evanado, A.; Carter-Monroe, N.; Kaikkonen, K. S.; Kortelainen, M. L.; Boucher, G.; Lagace, C.; Moes, A.; Zhao, X.; Kolodgie, F.; Rivadeneira, F.; Hofman, A.; Witteman, J. C.; Uitterlinden, A. G.; Marsman, R. F.; Pazoki, R.; Bardai, A.; Koster, R. W.; Dehghan, A.; Hwang, S. J.; Bhatnagar, P.; Post, W.; Hilton, G.; Prineas, R. J.; Li, M.; Kottgen, A.; Ehret, G.; Boerwinkle, E.; Coresh, J.; Kao, W. H.; Psaty, B. M.; Tomaselli, G. F.; Sotoodehnia, N.; Siscovick, D. S.; Burke, G. L.; Marban, E.; Spooner, P. M.; Cupples, L. A.; Jui, J.; Gunson, K.; Kesaniemi, Y. A.; Wilde, A. A.; Tardif, J. C.; O'Donnell, C. J.; Bezzina, C. R.; Virmani, R.; Stricker, B. H.; Tan, H. L.; Albert, C. M.; Chakravarti, A.; Rioux, J. D.; Huikuri, H. V.; Chugh, S. S. Identification of a sudden cardiac death susceptibility locus at 2q24.2 through genome-wide association in European ancestry individuals. *PLoS Genet.* **2011**, *7*, e1002158.
(29) Vidler, L. R.; Brown, N.; Knapp, S.; Hoelder, S. Druggability analysis and structural classification of bromodomain acetyl-lysine binding sites. *J. Med. Chem.* **2012**, *55*, 7346−7359.
(30) Ferguson, F. M.; Fedorov, O.; Chaikuad, A.; Philpott, M.; Muniz, J. R.; Felletar, I.; von Delft, F.; Heightman, T.; Knapp, S.; Abell, C.; Ciulli, A. Targeting low-druggability bromodomains: fragment based screening and inhibitor design against the BAZ2B bromodomain. *J. Med. Chem.* **2013**, *56*, 10183−10187.
(31) Philpott, M.; Yang, J.; Tumber, T.; Fedorov, O.; Uttarkar, S.; Filippakopoulos, P.; Picaud, S.; Keates, T.; Felletar, I.; Ciulli, A.; Knapp, S.; Heightman, T. D. Bromodomain-peptide displacement assays for interactome mapping and inhibitor discovery. *Mol. BioSyst.* **2011**, *7*, 2899−2908.
(32) Chung, C. W.; Dean, A. W.; Woolven, J. M.; Bamborough, P. Fragment-based discovery of bromodomain inhibitors part 1: inhibitor binding modes and implications for lead discovery. *J. Med. Chem.* **2012**, *55*, 576−586.
(33) Li, Y.; Sousa, R. Expression and purification of E. coli BirA biotin ligase for in vitro biotinylation. *Protein Expression Purif* **2012**, *82*, 162−167.
(34) Wang, P. J.; Page, D. C. Functional substitution for TAF(II)250 by a retroposed homolog that is expressed in human spermatogenesis. *Hum. Mol. Genet.* **2002**, *11*, 2341−2346.
(35) Xia, J.; Jia, P.; Hutchinson, K. E.; Dahlman, K. B.; Johnson, D.; Sosman, J.; Pao, W.; Zhao, Z. A meta-analysis of somatic mutations from next generation sequencing of 241 melanomas: a road map for the study of genes with potential clinical relevance. *Mol. Cancer Ther.* **2014**, *13*, 1918−1928.
(36) Savitski, M. M.; Fischer, F.; Mathieson, T.; Sweetman, G.; Lang, M.; Bantscheff, M. Targeted data acquisition for improved reproducibility and robustness of proteomic mass spectrometry assays. *J. Am. Soc. Mass Spectrom.* **2010**, *21*, 1668−1679.
(37) Bantscheff, M.; Hopf, C.; Savitski, M. M.; Dittmann, A.; Grandi, P.; Michon, A. M.; Schlegl, J.; Abraham, Y.; Becher, I.; Bergamini, G.; Boesche, M.; Delling, M.; Dumpelfeld, B.; Eberhard, D.; Huthmacher, C.; Mathieson, T.; Poeckel, D.; Reader, V.; Strunk, K.; Sweetman, G.; Kruse, U.; Neubauer, G.; Ramsden, N. G.; Drewes, G. Chemoproteomics profiling of HDAC inhibitors reveals selective targeting of HDAC complexes. *Nat. Biotechnol.* **2011**, *29*, 255−265.
(38) Middeljans, E.; Wan, X.; Jansen, P. W.; Sharma, V.; Stunnenberg, H. G.; Logie, C. SS18 together with animal-specific factors defines human BAF-type SWI/SNF complexes. *PLoS One* **2012**, *7*, e33834.

DOI: 10.1021/acs.jmedchem.5b00209
J. Med. Chem. 2016, 59, 1410−1424